Kinetics of the Isotopic Exchange Reaction between Carbon Monoxide and Carbon Dioxide*

By Teruo HAYAKAWA

(Received November 5, 1952)

Introduction

The kinetics of the exchange reaction between carbon monoxide and carbon dioxide have been investigated by Brandner and Urey,[1] using natural C^{13} isotope as a tracer, and by Norris and Ruben,[2] using radioactive C^{14} isotope as a tracer. The particular mechanism proposed by Brandner and Urey was based on the assumption of the presence of the activated forms of water and hydrogen (or activated hydrogen atom and hydroxyl radical) on the surface with the condition that the total amount of these molecules is constant.

The catalytic water gas reaction on the surface of a heated platinum wire in the region of 1,000°C.[3] is a famous one, and it is also generally known that water vapor and hydrogen are strongly adsorbed on quartz at these high temperatures. Nevertheless, unfortunately, the present author cannot accept their particular mechanism mentioned above for the following reasons:

(1) it seems somewhat doubtful that a considerable amount of water vapor, by which this exchange reaction was pronouncedly accelerated, was inevitably introduced and remained in the vessel,

(2) they have shown no direct evidence for the presence of the condition that the total amount of these activated molecules on the surface is constant.

On the other hand, Norris and Ruben proposed the mechanism of a bimolecular reaction between the two reactant species adsorbed on quartz. But, so far as their experimental results were concerned, it was not confirmed that the reaction is heterogeneous and catalytic.

Therefore, it seemed necessary for the present author to confirm the heterogeneity and the rate law of this exchange reaction.

Experimental

The natural C^{13} isotope, used in these experiments, was made by Prof. T. Titani[4] of Osaka University from the thermal diffusion of methane, and was fixed as silver carbonate. Carbon dioxide enriched in C^{13} was prepared from the thermal decomposition of silver carbonate and purified by several fractionations. Carbon monoxide was prepared from the decomposition of purified formic acid by heated phosphoric acid and purified by the usual method. During these purifications, water vapor was carefully prevented from entering into either of the sample gases. Argon was taken from cylinders, and was purified of oxygen and nitrogen by passage over hot copper turnings and then by calcium-arc discharges.

The reason for employing the C^{13} isotope (but not the O^{18} isotope) in these kinetic measurements has already been pointed out by Brandner and Urey.

A 55 cc. cylindrical quartz vessel (inner dia. 14 mm., length 35 cm.) was used in all runs. In testing for heterogeneity, the reaction vessel was packed with short sections of quartz tubing, whereby the surface-to-volume ratio was increased twofold approximately. The reaction vessel was connected to a glass high vacuum system through a water-cooled capillary graded seal, and closed by a capillary stopcock. Since the volume of the system was minimized by using 1.4 mm. capillary tubing throughout, the dead space between the reaction vessel and the stopcock was very small (about 0.8 cc.) compared with the volume of the reaction vessel, no correction for this was made for the results given in Table 1 and Table 2.

In these experiments the gases were premixed and introduced simultaneously into the hot quartz vessel, previously evacuated to $\approx 10^{-5}$ mm.Hg. and maintained in this vacuum during the period of 8-10 hrs. After the desired time the gases were pumped out and analysed by a mass spectrometer.

The mass spectrometer used in these experiments was of the 90° sector type, and the radius of curvature of the ion path was 13.0 cm. The details of this mass spectrometer were previously reported.[5] Though it seemed convenient to use

* This investigation was partly reported in the Annual Meeting of Chem. Soc. Japan (April, 1951).

(1) J. D. Brandner and H. C. Urey, *J. Chem. Phys.*, **13**, 351 (1945).

(2) T. H. Norris and S. Ruben, *J. Chem. Phys.*, **18**, 1595 (1950).

(3) C. N. Hinshelwood and C. R. Prichard, *J. Chem. Soc.*, **127**, 806 (1925).

(4) T. Titani and S. Horibe, *J. Chem. Soc. Japan*, **73**, 75 (1952).

(5) T. Hayakawa and T. Kambara, *J. Chem. Ind. Japan*, **54**, 310 (1951).

CHEMISTRY HALL LIBRARY

the same method with Urey and Brandner's, i.e., the direct connection of the reaction vessel to the ionization chamber of the mass spectrometer, the present author unfortunately could not use this method since the present instrument was designed for common use.

The reproducibility of this instrument for isotopic concentrations was ±0.01 (in atomic percentages); therefore, the good reproducibility was obtained in these usual runs. But, since the initial concentrations of $C^{13}O_2$ in these experiments were considerably low, the reproducibility in these several runs at the temperature of 710°C. was considerably poor. Herein, in these special runs, the average value of several measurements was adopted.

Result

The experimental results are summarized in Table 1 and Table 2, where the run numbers indicate the chronological order of the experiments.

Assuming that

(a) there is no isotope effect of C^{13}, and

(b) at equilibrium, the specific concentration of carbon dioxide (the percentage ratio, $C^{13}O_2$ to total CO_2) is equal to that of carbon monoxide,

the following first-order rate law expression[6]~[9] is easily obtained for the present exchange reaction,

$$C^{13}O_2 + C^{12}O \rightleftharpoons C^{13}O + C^{12}O_2$$

$$R = \frac{2.303\, p\mathrm{CO} \cdot p\mathrm{CO}_2}{(p\mathrm{CO}+p\mathrm{CO}_2)t} \log \frac{x_0 - x_\infty}{x - x_\infty} \qquad (1)$$

where R denotes the exchange rate, and x_0, x, x_∞, each denotes the specific concentration of carbon dioxide (the percentage ratio, $C^{13}O_2$ to total CO_2) at the time of initial, given, and equilibrium respectively.

The exchange rate, R, may also be expressed in the following form*

$$R = C \cdot f(p\mathrm{CO}_2) \cdot \varphi(p\mathrm{CO}) \qquad (2)$$

where C is a constant.

Fig. 1 gives a plot of rate *versus* carbon dioxide pressure at 900°C., at constant carbon monoxide pressure. Fig. 1 shows that the function $f(p\mathrm{CO}_2)$ is simply proportional to carbon dioxide pressure.

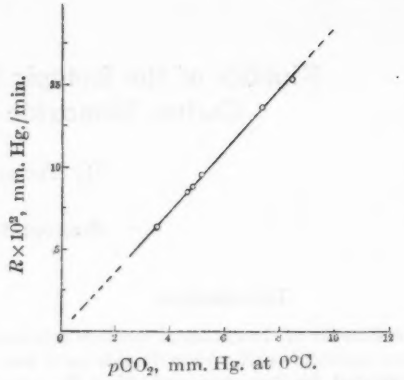

Fig. 1.—Dependence of exchange rate on carbon dioxide pressure at 900°C. $p\mathrm{CO}\approx8.5$ mm. Hg. at 0°C.

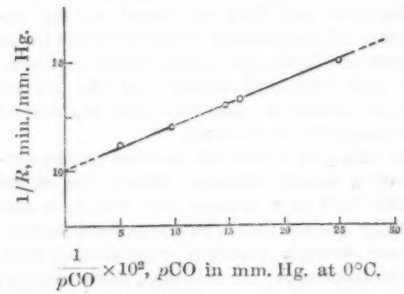

Fig. 2.—Dependence of exchange rate on carbon monoxide pressure at 900°C. $p\mathrm{CO}_2\approx3.9$ mm. Hg. at 0°C. $b=0.51$.

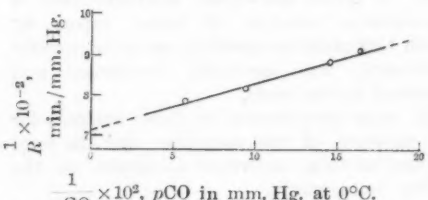

Fig. 3.—Dependence of exchange rate on carbon monoxide pressure at 770°C. $p\mathrm{CO}_2\approx3.5$ mm. Hg. at 0°C. $b=0.62$.

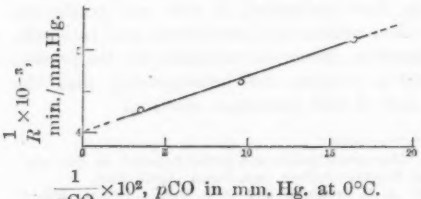

Fig. 4.—Dependence of exchange rate on carbon monoxide pressure at 710°C. $p\mathrm{CO}_2\approx4.8$ mm. Hg. at 0°C. $b=0.74$.

(6) H. A. C. McKay, *Nature*, **142**, 997 (1938).
(7) R. B. Duffield and M. Calvin, *J. Am. Chem. Soc.*, **68**, 557 (1946).
(8) J. W. Weigl and M. Calvin, *J. Chem. Phys.*, **17**, 210 (1949).
(9) K. S. Pitzer, *J. Chem. Phys.*, **17**, 1341 (1949).
* See, for example: H. A. C. McKay, *Nature*, **142**, 997 (1938).

On the other hand, a log-log plot of rate *versus* carbon monoxide pressure at 900°C., carbon dioxide pressure remaining constant, gives with a poorer approximation to a straight line, a slope of 0.2. So, the present author has adopted the following expression,

$$\varphi(p\mathrm{CO}) = C' \frac{p\mathrm{CO}}{1+b\cdot p\mathrm{CO}} \qquad (3)$$

where C' is a constant, and b is a constant depending on the temperatures.

Fig. 2, Fig. 3, and Fig. 4 indicate that this expression (3) is quite satisfactory for the present results. Then, the following rate law is obtained.

$$R = k \frac{p\mathrm{CO}\cdot p\mathrm{CO}_2}{1+b\cdot p\mathrm{CO}} \qquad (4)$$

Table 1

Exchange between CO_2 and CO (no additives).

Run	Time (min.)	Pressures (mm.Hg. at 0°C.) CO	Pressures (mm.Hg. at 0°C.) CO_2	Sp. concentrations CO_2 x_0	Sp. concentrations CO_2 x	Sp. concentrations CO_2 (x_∞) calcd.	Sp. concentrations CO y_0	Sp. concentrations CO y	k, $(k'\times 10^2)$	
Experiments at 710°±2°C.										
32	365	29.4	5.9	3.14	3.11	1.43	1.09	1.10	3.09×10^{-3}	
34	420	23.5	4.7	3.14	3.10	1.43	1.09	1.11	3.03	
35	510	10.3	6.0	3.12	3.08	1.82	1.08	1.09	3.01	
33	720	8.4	4.9	3.12	3.07	1.82	1.08	1.10	2.64	
38	810	6.1	5.9	3.13	3.08	2.10	1.09	1.16	2.96	
Experiments at 770°±2°C.										
41	54	17.6	3.5	3.14	3.10	1.43	1.09	1.10	2.10×10^{-4}	
43	60	6.2	3.5	3.12	3.08	1.82	1.08	1.12	2.44	
44	60	12.2	7.0	3.12	3.07	1.82	1.08	1.12	2.32	
45	180	9.4	5.4	3.12	2.99	1.82	1.08	1.20	2.70	
46	120	6.2	3.5	3.12	3.04	1.82	1.08	1.14	2.64	
49	30	8.9	4.3	3.15	3.13	1.78	1.09	1.10	2.38	
50	180	6.9	3.4	3.15	3.03	1.78	1.09	1.21	2.55	
Experiments at 900°±2°C.										
7	120	19.6	3.9	3.14	1.49	1.43	1.09	1.42	1.29×10^{-2}	(2.79)
9	270	9.4	4.0	3.14	1.68	1.68	1.09	1.69	—	
10	30	10.1	4.0	3.14	2.29	1.68	1.09	1.43	1.28	(2.91)
11	60	8.6	3.5	3.14	1.99	1.68	1.09	1.61	1.16	(3.03)
12	75	7.5	3.0	3.14	1.83	1.68	1.09	1.62	1.40	(3.04)
16	30	11.2	6.4	3.12	2.34	1.82	1.08	1.55	1.17	(3.06)
17	60	6.7	3.9	3.12	2.02	1.82	1.08	1.70	1.30	(3.12)
18	60	8.7	5.1	3.12	2.04	1.82	1.08	1.71	1.17	(2.96)
19	120	8.5	4.9	3.12	1.86	1.82	1.08	1.79	1.16	(2.90)
20	180	9.0	5.1	3.12	1.82	1.82	1.08	1.84	—	
21	90	8.4	4.8	3.12	1.90	1.82	1.08	1.77	1.25	(3.15)
23	30	8.7	8.4	3.13	2.46	2.10	1.09	1.67	1.14	(3.50)
24	60	5.7	5.5	3.13	2.28	2.10	1.09	1.93	1.02	(2.88)
26	150	7.2	7.0	3.13	2.10	2.10	1.09	2.11	—	
27	90	4.0	3.9	3.13	2.15	2.10	1.09	2.06	1.31	(3.36)
29	60	8.7	7.4	3.13	2.16	2.03	1.09	1.93	1.06	(3.56)
30	180	6.1	5.2	3.13	2.03	2.03	1.09	2.03	—	
Experiments at 900°±2°C. (Packed)										
54-P	15	6.7	4.5	3.15	2.48	1.90	1.08	1.53	2.03×10^{-2}	
55-P	30	6.3	4.2	3.15	2.22	1.90	1.08	1.68	1.82	
56-P	60	8.9	6.1	3.15	1.94	1.90	1.08	1.87	2.12	
57-P	45	8.7	5.9	3.15	2.03	1.90	1.08	1.82	1.87	
59-P	120	9.7	6.5	3.15	1.90	1.90	1.08	1.91	—	

Accordingly, the equation (1) becomes

$$\frac{2.303\,p\mathrm{CO}\cdot p\mathrm{CO}_2}{(p\mathrm{CO}+p\mathrm{CO}_2)\,t}\log\frac{x_0-x_\infty}{x-x_\infty}=k\frac{p\mathrm{CO}\cdot p\mathrm{CO}_2}{1+b\cdot p\mathrm{CO}} \qquad (5)$$

This equation (5) has been used to calculate the values of k given in Table 1 and Table 2. It is seen that the agreement among all the runs is fairly good.

The average k values (unpacked, non-additives) have been plotted in Fig. 5 as the logarithm of k *versus* $1/T$. The fact that the points give a reasonable approximation to a straight line suggests that there is but one exchange mechanism in this temperature range. The slope of this plot indicates an apparent activation energy of 73 kcal./mol., and this value is in good agreement with the value of 77 kcal./mol. obtained by Norris and Ruben.

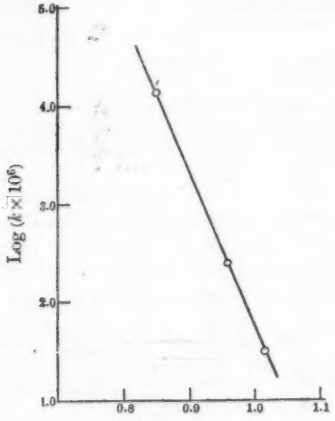

Fig. 5.—Temperature dependence of rate constant.

In order to test for heterogeneity, the reaction vessel was packed with short sections of quartz tubing, thus increasing the surface-to-volume ratio twofold approximately. From the results shown also in Table 1, it is clear that the rate of this exchange reaction is considerably increased by packing, though this increase in the rate is not correctly proportional to the surface-to-volume ratio. And this effect of packing is, as a tendency, similar to the results obtained by Brandner and Urey, but it is inconsistent with the results of Norris and Ruben.

The present results on the effect of water and argon are indicated in Table 2. As seen in Table 2, the addition of argon has no influence (rather slight retardation) on this reaction within the experimental error. On the other hand, the addition of water apparently indicates a pronounced acceleration. But as discussed below, this apparent acceleration caused by adding water is not real.

Discussion

From the facts that the reaction is considerably retarded by carbon monoxide and is

Table 2

The Influence of Argon and Water (at 900°C.)

(1) Argon addition (10 vol. %)

Run	Time (min.)	Pressures (mm.Hg. at 0°C.)			Sp. concentrations					$k\times10^2$
					CO_2			CO		
		CO	CO_2	Ar	x_0	x	(x_∞) cal.	y_0	y	
51	15	11.1	2.0	1.3	3.14	2.62	1.41	1.09	1.18	1.04
52	30	8.2	1.5	1.0	3.14	2.39	1.41	1.09	1.24	1.02
53	60	16.8	3.0	2.0	3.14	1.97	1.41	1.09	1.31	0.90

(2) Water addition ($x_0=3.14$, $y_0=1.09$).

Run	Time (min.)	Initial pressures (mm.Hg. at 0°C.)				x	Composition $(CO_2)/(CO)+(CO_2)$		$\frac{(C^{13}O_2)}{(C^{13}O_2)_0}$
		CO	CO_2	H_2O			initial (t_0),	final (t),	
62	15	8.6	3.5	1.8		1.99	0.29	0.33	0.72
63	30	10.1	4.0	2.1		1.71	0.28	0.36	0.70
(10)	(30)	(10.1)	(4.0)	(0)	(≈15%)	(2.29)			(0.74)
65	45	7.5	3.1	1.5		1.67	0.29	0.36	0.66
(12)	(75)	(7.5)	(3.0)	(0)		(1.83)			(0.58)
67	15	8.4	3.6	1.0	(≈8%)	2.21	0.30	0.34	0.80
68	30	9.8	4.3	1.2		1.98	0.30	0.35	0.73
70	15	8.6	3.5	2.4	(≈20%)	1.68	0.29	0.37	0.68
72	45	7.6	3.2	2.2		1.59	0.30	0.38	0.63

markedly accelerated by packing, it seems reasonable to consider that this exchange reaction is heterogeneous and catalytic, as it was partly suggested by Urey and Brandner. In the experiments of Norris and Ruben on this question of heterogeneity, the surface-to-volume ratio was increased sixfold by packing, but the k values obtained by them indicated almost no effect. Though they considered that their data might indicate a reaction partly homogeneous, it seems rather reasonable for the present author to consider their data indicating much lower catalytic activity of their quartz. This is partly based on the fact that their k values at 900°C. are very small compared with that of the present author's, and is also partly based on the reasons discussed later.

As generally discussed by Morita,[10] the relations expressed in equation (1) and (2) are, in themselves, well explained whenever the rate-determining process of the catalytic exchange reaction is the direct exchange between the two reactant species or the adsorption (or the desorption) of any one of the reactants. But, from the fact that the present results are well satisfied by the rate law expression (4), it seems reasonable for the present author to believe that this exchange reaction is obeyed in any one of the following mechanisms.

Mechanism (1)—

$$C^{13}O_2 \text{ (gas phase)} + C^{12}O \text{ (adsorbed)} \rightleftarrows C^{13}O \text{ (adsorbed)} + C^{12}O_2 \text{ (gas phase)}$$

$$R = k \cdot p\mathrm{CO}_2 \cdot \varphi(\mathrm{CO})$$

where $\varphi(\mathrm{CO})$ denotes the adsorbed amount of carbon monoxide.

According to this mechanism (1), the reaction is a bimolecular exchange between the strongly adsorbed carbon monoxide molecule and the carbon dioxide molecule in the gas phase. The function $\varphi(\mathrm{CO})$ may be determined from the adsorption state of carbon monoxide, and in the present experiments it must satisfy the form $c' \cdot p\mathrm{CO}/1 + b \cdot p\mathrm{CO}$.

Therefore, in order to test for this problem, it was necessary to determine the adsorption states of the two reactant species at the temperatures of these experiments, using the same quartz vessel.

The present observations using a constant volume method[11] have been plotted in Fig. 6. Each line in Fig. 6 corresponds to each separated adsorption isotherm at 900°C. Fig. 6 shows that the adsorption of carbon monoxide on this quartz surface is considerably large, especially in comparison with that of carbon dioxide, and the adsorbed amount of each reactant is simply proportional to its pressure approximately.

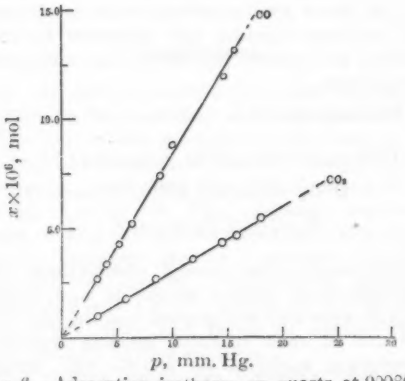

Fig. 6.—Adsorption isotherm on quartz at 900°C.

Then, according to mechanism (1), the present adsorption experiments must result in the rate law

$$R = k \cdot p\mathrm{CO} \cdot p\mathrm{CO}_2$$

However, unfortunately, thus obtained rate law is inconsistent with the results of this exchange reaction expressed in equation (4).

But, since the present observations in testing for the adsorption of carbon monoxide were obtained for the total surface of the reaction vessel and in this condition the adsorption of carbon monoxide was stronger than that of carbon dioxide at this high temperature, it seems also probable that the adsorption of carbon monoxide on the active surfaces for this reaction may be rather strong and may obey the usual Langmuir's isotherm.

$$\varphi(\mathrm{CO}) = C' \cdot p\mathrm{CO}/1 + b \cdot p\mathrm{CO}$$

Therefore, the present results of this exchange reaction are well explained by mechanism (1).

On the other hand, since it is probable to think of the present exchange reaction as an oxidation of carbon monoxide by carbon dioxide, many studies[12]~[15] of the carbon

(10) N. Morita, This Bulletin, **15**, 166 (1940); *J. Chem. Soc. Japan*, **44**, 62 (1941).

(11) See, for example: A. F. Benton and T. A. White, *J. Am. Chem. Soc.*, **52**, 2325 (1930); W. J. C. Orr, *Proc. Roy. Soc.*, **A173**, 349 (1939).

(12) M. Bodenstein and F. Ohlmer, *Zeit. Phys. Chem.*, **53**, 163 (1905).

(13) A. F. Benton and T. L. Williams, *J. Phys. Chem.*, **30**, 1487 (1921).

(14) F. Handman, H. W. Thompson and C. N. Hinshelwood, *Proc. Roy. Soc.*, **A137**, 87 (1932).

(15) Y. Kondo and O. Toyama, *Rev. Phys. Chem, Japan*, **13**, 166 (1939).

monoxide-oxygen reaction in quartz must show certain similarities to the present one.

These studies have shown that this dry and non-explosive oxidation at the temperatures lower than 800°C. is heterogeneous and that strongly adsorbed carbon monoxide and rather weakly adsorbed oxygen interact each other.

Although the results of these studies mentioned above are inconsistent with mechanism (1), we must consider the difference between oxygen and carbon dioxide in the adsorptive properties.

Mechanism (2)—

$$C^{12}O\ (\text{adsorbed}) + C^{13}O_2\ (\text{adsorbed}) \rightleftarrows C^{12}O_2\ (\text{adsorbed}) + C^{13}O\ (\text{adsorbed})$$

$$R = C \cdot f(pCO_2) \cdot \varphi(pCO)$$

According to the present observations, the adsorptions of carbon monoxide and carbon dioxide were both rather weak and the adsorbed amount of each reactant in each separated adsorption isotherm at 900°C. was simply proportional to its pressure. However, since these results were obtained for the total surface of the quartz vessel, when each reactant is adsorbed on each different surface (without mutual displacement) and the adsorption of carbon monoxide on the active surfaces for this reaction is moderate the rate of this exchange reaction follows[16]

$$R = k \cdot \frac{pCO}{1 + b \cdot pCO} \cdot pCO_2$$

This rate law coincides well with expression (4).

Moreover, since the catalytic activities of various kinds of quartz vary considerably when the adsorptions of carbon monoxide and carbon dioxide on the different active surfaces are both moderate, the rate of this exchange reaction seems to follow[17]

$$R = k \cdot \frac{pCO}{1 + b \cdot pCO} \cdot \frac{pCO_2}{1 + b' \cdot pCO_2} \approx k \cdot pCO^m \cdot pCO_2{}^n$$

The rate law thus obtained is in good agreement with the results of Norris and Ruben ($m \approx 0.7$, $n \approx 0.35$).

On the other hand, one may derive the similar rate law when two reactant species are both moderately adsorbed on the same surface and $1 \gg (b \cdot pCO)^2$, $(b' \cdot pCO_2)^2$,

$$R = k \cdot \frac{pCO \cdot pCO_2}{(1 + b \cdot pCO + b' \cdot pCO_2)^2} \approx k \cdot pCO^m \cdot pCO_2{}^n$$

However, unfortunately, the present results of this exchange reaction are unexplained by the adsorptions of two reactant species on the same surface. And from the fact that the value of the apparent activation energy of this exchange reaction obtained by the present author is in good agreement with that of Norris and Ruben, it seems probable that the reaction, both in the present author's and in that of Norris and Ruben, obeys a similar mechanism.

From these reasons mentioned above, though the present results are well explained by both mechanisms (1) and (2), the latter seems more probable to the present author.

In both mechanism (1) and (2), it is also necessary to ascertain the influence of the side reaction on the quartz surface.

$$2CO \rightleftarrows CO_2 + C$$

This reaction on a nickel catalyst was investigated in detail by Rhi.[18]

The present results in testing for this reaction, using the same quartz vessel, are shown in Table 3. Table 3 shows that this reaction slightly occurs at the temperatures of these experiments. However, as it was also suggested by Brandner and Urey, since the pressure of the gas mixture and the percentage of carbon monoxide was not sufficiently high in any present exchange experiment to cause deposition of massive carbon on the walls of the quartz vessel, the influence of this side reaction on the present exchange reaction appears to be very small.

Table 3

The Decomposition of Carbon Monoxide (at 900°C.).

Initial Pressure pCO (mm.Hg. at 0°C.)	Time t (min.)	CO_2, formed (vol. %)
10.9	60	0.7
10.7	180	1.0
21.2	60	1.2
21.2	120	1.5
30.6	30	1.1
30.6	63	1.9
30.9	120	2.4

The mechanism suggested by Brandner and Urey is an excited water gas reaction on the walls of the quartz vessel.

(16) See, for example: G. M. Schwab, *Zeit. Elektrochem.*, **35**, 573 (1929).
($2CO + O_2 = 2CO_2$, on SiO_2).

(17) See, for example: C. R. Prichard and C. N. Hinshelwood, *J. Chem. Soc.*, **127**, 1546 (1925).

(18) T. Rhi, *Rev. Phys. Chem. Japan*, **8**, 89 (1934); **10**, 200 (1936).

$$H_2 = H_2^*$$
$$C^{13}O_2 + H_2^* \rightleftarrows C^{13}O + H_2O^*$$
$$H_2O^* \rightarrow H_2O$$
$$(H_2^*) + (H_2O^*) = \text{constant}$$

They considered that their mechanism might be supported, though it was not entirely free of difficulties, by the fact that the exchange rate was markedly accelerated by adding hydrogen or water vapor.

As has been mentioned, the study of the catalytic water gas reaction on the surface of a heated platinum wire is a famous one.

And it seems also probable that hydrogen and water vapor are strongly adsorbed on quartz at the temperatures of these experiments and, then, they cause a marked acceleration of this exchange reaction.

Indeed, as seen in Table 2, since the values of x (percentage ratio, $C^{13}O_2$ to total CO_2) are markedly decreased in these experiments, the addition of water apparently causes a pronounced acceleration of this exchange reaction. However, it must be noticed that in each run of adding water the final concentration of carbon dioxide is also considerably increased and, then, this acceleration is only apparent and not true. The true acceleration caused by adding water must be much smaller than this, and may be measured by $(C^{13}O_2)/(C^{13}O_2)_0$ in Table 2, where $(C^{13}O_2)_0$ and $(C^{13}O_2)$ each denotes the concentration of $C^{13}O_2$ at the initial and given time respectively. Accordingly, the present results shown in Table 2 indicate that the true acceleration is somewhat increased with the water contents. This would seem inconsistent with Brandner and Urey's important assumption in their mechanism, because their mechanism is based on the assumption that the surface is completely covered by these molecules of H_2^* and H_2O^* and that the total amount of these molecules is constant. And it seems also very difficult for the present author to suppose that in each exchange experiment of no additives the considerable amount of water vapor remained in the reaction vessel. Moreover, unfortunately, Brandner and Urey's mechanism fails to explain the fact of the exchange rate in the present experiments obeying expression (4).

The present author calculated the rate constant, k', on the basis of Brandner and Urey's rate law and mechanism. Although each value of k' (at 900°C.) given in Table 1 apparently indicates rather good agreement, this may be attributed to the fact that the value of $1 + b \cdot p\mathrm{CO}/p\mathrm{CO} + p\mathrm{CO}_2$ in the present experiments at 900°C. is not very different from the others.

From these reasons it seems inevitable for the present author to consider that the mechanism suggested by Brandner and Urey (a excited water-gas reaction) is, in itself, a different reaction from the present exchange reaction, though it contains many interesting suggestions.

Conclusions

It has been concluded that this exchange reaction is heterogeneous and catalytic.

The rate of this reaction has the form of a product of adsorption isotherms. The probable mechanism—and then the probable rate determining process—of this exchange reaction seems to be a bimolecular exchange (oxidation) reaction between the two reactant species adsorbed on quartz. Although a similar mechanism was already suggested by Norris and Ruben, they had failed to confirm the heterogeneity of this reaction.

The present results are somewhat different from those of Norris and Ruben. In the present experiments, it seems probable to consider that each reactant is adsorbed on each different surface and the adsorption of carbon monoxide on the active surfaces for this exchange reaction is moderate, but carbon dioxide is rather weakly adsorbed.

The results obtained by Norris and Ruben suggest to us that the adsorption of the two reactant species in their experiments are both moderate and not very different.

It is supposed that the observed difference between the results of Norris and Ruben and that of the present author may be attributed to the difference in the catalytic activity of quartz.

The present exchange reaction is somewhat accelerated by adding water. Probably it may depend on the occurrence of the water gas reaction,

$$CO_2 + H_2 \rightleftarrows CO + H_2O$$

Although Brandner and Urey proposed this mechanism (an excited water gas reaction) for the present exchange reaction, their mechanism does not satisfy the present results of this exchange reaction.

Therefore, so far as the present experiments are concerned, the present author considers that the reaction mechanism is fundamentally different in the presence and in the absence of water vapor or hydrogen.

The author wishes to express his grateful

thanks to Professor T. Titani of Osaka University who kindly offered his precious sample of C^{13} isotope and also many helpful suggestions on this problem, and to Professor O. Toyama of Naniwa University for his kind discussions.

The author is also greatly indebted to Dr. T. Kambara of the Central Laboratory of Hitachi Factory for using his mass spectrometer.

Department of Chemistry, Faculty of Education, Naniwa University, Sakai, Osaka

---

Dichroisms of Benzene Rings. IV. The Dichroisms of Diphenyldiacetylene and Naphthazarine

By Kazuo NAKAMOTO

(Received September 27, 1952)

Introduction

In the former papers of this series,[1] remarkable dichroism of the benzene ring has been found in common aromatic crystals and molecular compounds. From the viewpoint of quantum mechanics, however, the triple bond is expected to show more remarkable dichroism than the double bond because the former has two π-electrons in each carbon atom. So it is of interest to measure the dichroism of the triple bond and to compare it with that of the benzene ring.

In the present study, the dichroism of diphenyldiacetylene whose crystal structure had been perfectly determined by X-ray analysis has been measured quantitatively in the ultraviolet region. The result seems noteworthy, indicating remarkable dichroism of the triple bond independent of the dichroism of the benzene ring.

Of particular interest in the field of molecular structure is the problem of determining whether naphthazarine, 5,8-dihydroxy-1,4-naphthoquinone, exists as a molecular compound similar to quinhydrone or as the monomer in crystalline state. The result of the dichroism measurement has led us to the conclusion that a formation of molecular compound is not probable so far as the assumed orientation of molecules is correct.

Experimental

Materials.—(1) Diphenyldiacetylene—Colourless acicular crystals were obtained by recrystallization from an alcoholic solution. M. p. 87°. Monoclinic system. Straight extinction. Dichroism can not be observed with the naked eye. (2) Naphthazarine—The Friedel-Crafts synthesis between hydroquinone and maleic anhydride[2] was employed for the preparation of this substance. Recrystallization from a ligroin solution produced violet needle crystals similar to quinhydrone. Since naphthazarine slowly decomposes on heating in the air, its melting point was identified as the diacetate (m. p. 192°). Monoclinic system. Straight extinction. Thin crystals show slight dichroism; rose, when viewed with linearly polarized light whose electric vector vibrates parallel to the c-axis (needle axis), and rose red, with the light vibrating parallel to the b-axis.

Measurements.—Dichroisms of the crystals were measured quantitatively by the microscopic method with microcrystals as described before[1]. Spectra of the alcoholic solutions were measured by photographic method using the rotatory sector. In each graph, the ordinates, α and ε denote absorption coefficient per mm. of the crystal, and molar extinction coefficient of the solution, respectively.

Results and Discussion

(1) **Diphenyldiacetylene.**—In 1940, Wiebenga[3] studied the crystal structure of diphenyldiacetylene and succeeded in its Fourier analysis. According to his result, planar molecules of diphenyldiacetylene are piled up along the c-axis, making their molecular planes almost parallel to the a-axis and inclined by an angle of 25° referred to the b-axis.

(1) K. Nakamoto, *J. Am. Chem. Soc.*, **74**, 390, 392 and 1739 (1952).

(2) K. Zahn and P. Ochwat, *Ann.*, **462**, 81 (1928).

(3) E. H. Wiebenga, *Z. Krist.*, **102**, 193 (1940).

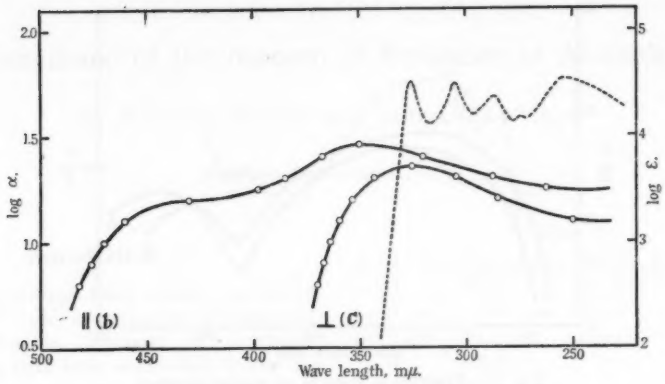

Fig. 1.—Absorption spectra of diphenyldiacetylene.

Absorption spectra by linearly polarized light with the electric vectors vibrating parallel to the b- and c-axes, respectively, are recorded in Fig. 1. Numerical data characterizing these spectra are given in Table 1.

Table 1

	1st band (acetylene band)		2nd band (benzene band)	
	$\lambda_{max.}$	$\log \alpha_{max.}$	$\lambda_{max.}$	$\log \alpha_{max.}$
b-abs.	430	1.20	350	1.45
c-abs.			325	1.30

The absorption spectrum of diphenyldiacetylene in an alcoholic solution is also given in Fig. 1 (dotted line). As is clearly shown in the spectra of diphenylpolyin series,[4] the four distinct bands at 326, 305.3, 287.4 and 275.5 mμ are the absorptions due to the acetylene group in the molecule. The next broad band appeared at 255 mμ is attributed to the absorption resulting from the π-electrons of the benzene rings.

As is seen above, the acetylene band is bathochromic in respect to the benzene band. This relation may hold also for the spectra in crystalline state. In the b-absorption of crystalline state, therefore, the first band at 430 mμ and the second band at 350 mμ are concluded to be due to the acetylene group and the benzene ring, respectively. In the c-absorption, however, only one maximum which may be ascribed to the benzene band appears at 325 mμ, because the acetylene band is too weak in this polarized light. Nevertheless, we can expect that the b-absorption of the acetylene band is bathochromic and hyperchromic to the c-absorption from experimental analogy between the dichroism of the benzene ring and that of the acetylene group.

Comparing the result of X-ray analysis with the above spectroscopic discussion, we may conclude that the absorption parallel to the acetylene bond and the benzene rings is bathochromic and hyperchromic to the absorption perpendicular to them. Thus the acetylene group shows the same dichroic property as the benzene ring, except the former indicates more remarkable dichroism than the latter.

(2) **Naphthazarine.**—It has been a subject of much discussion both experimental and theoretical to decide whether naphthazarine exists as a molecular compound similar to quinhydrone or as the monomer in crystalline state. In an attempt to solve this problem, measurements of the dichroism of naphthazarine crystals have been made in the visible and ultraviolet region. As to the X-ray study on this crystal, Palacios and Salvia[5] have measured only the dimension of its unit cell and no further detailed study has been undertaken.

According to their result, the unit cell of naphthazarine crystal[6] is as follows:

$$a=3.85,\ b=8.02,\ c=14.5\ \text{Å}.\ \beta=97°6'$$

Considering that a is nearly equal to ordinary

(4) M. Nakagawa et al., *J. Chem. Soc. Japan*, **72**, 561 (1950); **73**, 141 (1951).
For another example, see W. D. Celmer and I. A. Solomons, *J. Am. Chem. Soc.*, **74**, 384) (1952).

(5) J. Palacios and R. Salvia, *Anales. soc. espan. fis. quim.*, **32**, 49 (1934).

(6) Naphthazarine has at least two modifications. The one was recently used by Rogers for the measurement of magnetic anisotropy (*J. Am. Chem. Soc.*, **69**, 1536 (1947)). The other was studied by Palacios and Salvia as stated above, and used here for the dichroism measurement.

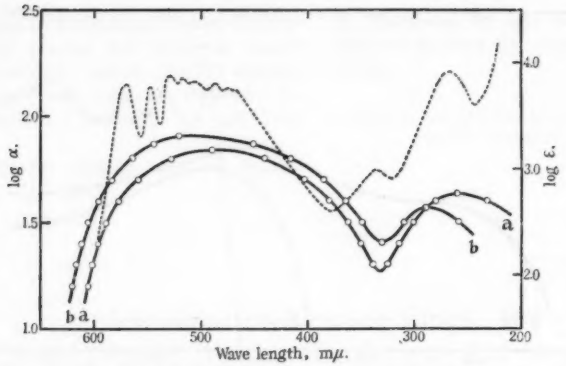

Fig. 2.—Absorption spectra of naphthazarine.

distance which separates aromatic layers, it seems probable that the molecules are piled up along the a-axis. Thus, the absorption spectra by linearly polarized lights with the electric vector vibrating parallel to the a- and the b-axes have been measured. Their curves and numerical data are given in Fig. 2 and Table 2, respectively.

Table 2

	λmax.	log αmax.	λmax.	log αmax.
a-abs.	490	1.84	250	1.64
b-abs.	510	1.92	290	1.57

The absorption spectrum of naphthazarine in an alcoholic solution is also shown in Fig. 2 (dotted line). It has a broad intense band with vibrational structure between 570~470 mμ, which may be ascribed to the absorption principally due to the π-electron system in the molecule. The first bands at 510 and 490 mμ in crystalline state coincide with the above π-band in liquid state. Therefore we conclude that the π-band is bathochromic and hyperchromic in the b-absorption rather than in the a-absorption.

Conforming the probable orientation of molecules with the above result, we can reach the conclusion that the absorption parallel to the molecular plane is bathochromic and hyperchromic to the absorption perpendicular to it. In other words, the general rule about the dichroism of molecular compounds does not hold here and naphthazarine indicates similar dichroic property to common aromatic crystals. This conclusion suggests to us that a possibility of forming a molecular compound like quinhydrone is not probable in the present case.

If there exists any overlap of the π-orbitals that are thrust out perpendicularly from each molecular plane, the feature of the spectra would be expected to produce a marked change.[1]

Summary

Absorption spectra of diphenyldiacetylene and naphthazarine in crystalline state as well as in solution have been measured quantitatively in the visible and ultraviolet region. In the former compound, it has been found that the acetylene group indicates similar dichroic property to the benzene ring except for the fact that the dichroism of the former is more remarkable than that of the latter. From the dichroic property of naphthazarine, it has been concluded that the substance exists as the monomer and does not form the molecular compound like quinhydrone even in crystalline state.

The author wishes to express his sincere thanks to Prof. R. Tsuchida for his kind guidance and encouragement throughout this work. Appreciation is also expressed to Dr. Nakagawa for the gift of diphenyldiacetylene used in this work.

Department of Chemistry, Faculty of Science, Osaka University, Osaka

Estimation of the Amount of Hydration of Alcohols

By Tunetaka SASAKI and Tatuya YASUNAGA

(Received December 11, 1952)

Introduction

The present authors have already calculated the volume of water of hydration (abbreviated to call hydration volume) of inorganic ions, assuming that both solute and hydration water are incompressible, and they have confirmed that such an assumption was permissible, for the values thus obtained ran parallel with the heat of hydration and electrostriction.[1] A similar calculation cannot however be applied in the case of hydration of alcohols in aqueous solution because the incompressibility of solute and hydration water, especially the latter, cannot be assumed. This comes chiefly from the difference between a strong interaction of ion~water dipole in the case of the aqueous electrolyte solution and a weak interaction of dipole~dipole or of hydrogen bond frequently pointed out to form in the case of aqueous solution of nonelectrolyte.[2] This problem can however be attacked from a somewhat different direction if we take up the sound velocity in aqueous solution instead of the compressibility.

Principle of Calculation

Recently, Rao[3] has pointed out that the function,

$$v^{1/3}M/D=V \qquad (1)$$

where v is the velocity of sound, M the molecular weight, and D the density, is a constant, characteristic of a pure liquid, and is additive and constitutive in that it may be computed by summing increments assigned to atoms and bonds. Lagemann and Corry[4] however proposed an alternative procedure for computing this constant, that is, there is an additivity only of what they choose to call "*bond velocities*" shown in the following table.

Table 1

Bond	Bond Increment	Bond	Bond Increment
C—H	95.2	C—Cl	230
C—C	4.25	C=C	129
C—O	34.5	C=O	186
O—H	99.0		

Now, we assume that this additivity rule also applies in the case of an ideal solution, just as the similar rule applies in the case of molecular polarization. Thus for an ideal solution

$$V_1N_1+V_2N_2=v^{1/3}\frac{M_1N_1+M_2N_2}{D} \qquad (2)$$

is assumed to hold, where N represents the molal fraction. In the case of an aqueous alcohol solution however, the above relation does not hold, because the solution is not a mere mixture of alcohol and water molecules. We may rather assume a ternary mixture composed of alcohol, bound or hydration water and free or solvent water for such a solution. Then we get the following equation instead of the equation (2),

$$V_1(N_1-x)+V_2N_2+V_1'x=v^{1/3}\frac{M_1N_1+M_2N_2}{D} \qquad (3)$$

where x and V_1' are the molal fraction and molecular sound velocity of hydration water respectively. From the equation (3), we obtain the amount of hydration per mole solute,

$$\frac{x}{N_2}M_1=\left[v^{1/3}\frac{M_1N_1+M_2N_2}{D}-(V_1N_1+V_2N_2)\right]\times M_1/V_1'V_1)N_2 \qquad (4)$$

Experimental Results and Discussions

First of all we checked the validity of the above mentioned additivity rule of bond velocity for water which differs widely in nature from other organic liquids checked by Lagemann and Corry.[4] We could confirm that

(1) T. Yasunaga and T. Sasaki, *J. Chem. Soc. Japan*, **72**, 316 (1951).
(2) H. S. Frank and M. W. Evans, *J. Chem. Phys.*, **13**, 507 (1945), A. L. Robinson, *J. Chem. Phys.*, **14**, 588 (1946).
(3) M. R. Rao, *J. Chem. Phys.*, **9**, 682 (1941).
(4) R. T. Lagemann, and J. E. Corry, *J. Chem. Phys.*, **10**, 759 (1942).

Table 2

Fraction by volume of heptane in mixture at 20°C.	Sound Velocity m./sec.	Density$^{20}_{4}$	$V_1N_1+V_2N_2$	$v^{1/3}(M_1N_1+M_2N_2)/D$	% error
0.000	1039.4	0.6278	1163.2	(1163.2)	0.00
0.223	1058.4	0.6416	1245.6	1244.3	0.10
0.409	1082.3	0.6519	1314.3	1311.9	0.18
0.607	1107.1	0.6622	1387.5	1392.1	0.33
0.806	1130.1	0.6737	1461.0	1463.1	0.14
1.000	1152.4	0.6849	1532.7	(1532.7)	0.00

the equation (1) gave a numerical value of 201 for V of water while we obtained the value of 198 as twice the value of OH bond velocity. Thus we can safely apply the additivity rule for at least the pure liquids concerned.

Further we made an experimental confirmation of the equation (2). Fortunately we found data available for this purpose which has been offered by Jacobson[5] for the case of the mixture of heptane and pentane. In this case also, as is shown in Table 2, an excellent agreement can be seen between $V_1N_1+V_2N_2$ and $v^{1/3}(M_1N_1+M_2N_2)/D$.

We then proceeded to study the validity of the equation (3) or (4), for the case of aqueous alcohol solutions.

Here we employed the fixed frequency type acoustic interferometer reported in a previous paper[6] to measure the sound velocity in a liquid mixture. The sound velocity measured was shown as a linear function of concentration in Fig. 1. From this figure, we can obtain the value for v of the equation (4), for a given concentration. To estimate the value V_1' in the equation (4), we assumed that hydration of alcohol is chiefly due to the hydrogen bridge between alcohol and water molecules, and approximated the hydration water to be ice. The value V_1' can then be calculated from the equation (1) using the values for ice. Thus we obtained $V_1'=259.7$.

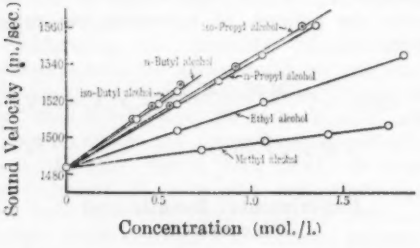

Fig. 1.—Sound velocity of aqueous alcohol solution at 20°C.

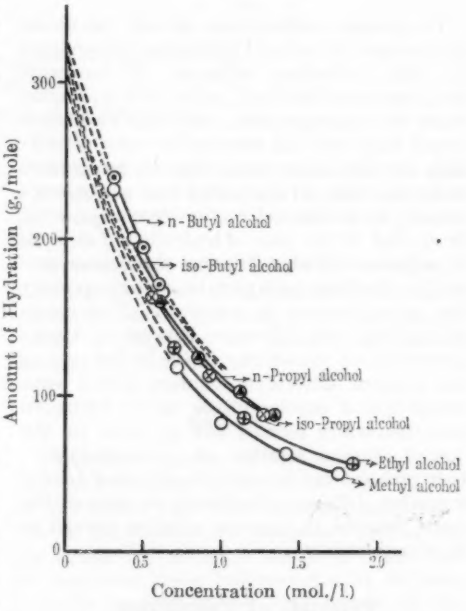

Fig. 2.—Amount of hydration per mole of alcohol at 20°C.

Using these values we calculated the amount of hydration as a function of concentration, from the equation (4). The results were shown in Fig. 2. In this figure we note a set of parallel curves for alcohol homologues. We fan also see that the amount of hydration increases with the number of carbon atoms in a molecule at constant concentration, and decreases with the concentration for one and the same alcohol which is in accord with the general behavior of the hydration. Further we compared the above value of amount of hydration (at 1 mol/liter concentration) with the known value of heat of hydration which was calculated for alcohols by Butler.[7] A

(5) B. Jacobson, *Arkiv Kemi.*, **2**, 177 (1950).
(6) T. Yasunaga, *J. Chem. Soc. Japan*, **72**, 87 (1951).
(7) J. A. V. Butler, "Structure and Molecular Forces in (a) Pure Liquids and (b) Solution", *Faraday Society*, 229 (1935).

fairly good proportionality between these quantities is noticed in Fig. 3. The fact again leads us to the conclusion that the amount of hydration hereby obtained is the quantity closely related to the actual amount of water of hydration.

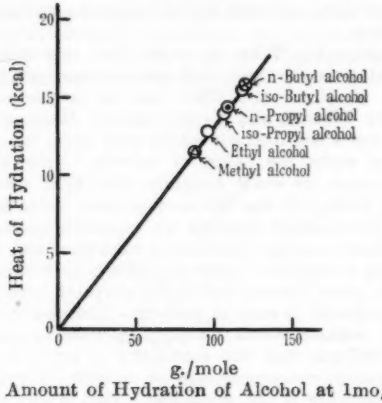

Fig. 3.—Relation between heat of hydration and amount of hydration at 1 mol/l.

Summary

The amount of hydration for alcohols in aqueous solution was estimated, assuming that the molecular sound velocity of a solution can be calculated from that for each constituent of the solution and their molal fraction, thereby regarding the water of hydration as the third component different from the free solvent and rather resembling ice as far as the sound velocity is concerned. The quantities thus calculated showed the general behavior of hydration water and also proved to be proportional to the heat of hydration.

A part of the cost of this study has been defrayed from the Scientific Research Expenditure of the Ministry of Education given to one of the authors.

Department of Chemistry, Faculty of Science, Kyushu University, Fukuoka.

On the Relation between Viscosity and Critical Micelle Concentration of Detergent Solutions*

By Naoyasu SATA and Kiyoshi TYÛZYÔ

(Received August 2, 1952)

Introduction

The viscosity of detergent solutions has been investigated for a long time, but almost all investigations before 1935 were carried out in the region of concentrated solutions owing to the insufficient knowledge about the structure of micelles in this period.(1) Thereafter, there was also no research which dealt with the relation between viscosity and micelle-structure. In 1939, Hess, Philippoff and Kiessig found a method of determining critical micelle concentration (CMC) of soap solutions from their viscosity and measured viscosities of several soap solutions for a wide range of concentration.(2) Although this is a remarkable investigation, it did not yet try to discuss the size and shape of micelle from viscosity data, because the systematic investigation of micelle-structure began gradually at that period. However, after 1940, new interesting phenomena (e. g., solubilization,(3) spectral dye(4)) were found and several new physical methods (e. g., long spacing X-ray diffraction,(5) light scattering(6)) were applied to the micelle-investigation, so that knowledges concerning micelle increased suddenly. We can remember the

* Part of this paper was presented at the 5th Annual Meeting of the Chemical Society of Japan, April, 1952 in Tokyo.

(1) E. L. Lederer, "Kolloidchemie der Seifen" 1932, S. 141.

(2) K. Hess, W. Philippoff and H. Kiessig, *Kolloid-Z.*, **88**, 40 (1939).

(3) J. W. McBain and R. C. Merrill, *Ind. Eng. Chem.*, **34**, 915 (1942).

(4) M. L. Corrin and W. D. Harkins, *J. Am. Chem. Soc.*, **69**, 679 (1947).

(5) W. D. Harkins, R. W. Mattoon and M. L. Corrin, ibid., **68**, 220 (1946).

(6) P. Debye, *J. Colloid Sci.*, **3**, 407 (1948).

discovery of 1st and 2nd CMC, theories of spherical, cylindrical and lamellar micelle, etc.

Therefore it seems necessary to review the existing many viscosity data again, under the light of the new structural theory of micelles.

We want to remark first the superiority of the viscosity-method in comparison with other methods of CMC-determination; secondly describe our new simple method of determining 1st and 2nd CMC from viscosity and finally discuss the relation between molecular weight of micelle and characteristic constants concerning viscosity which we have newly discovered.

Comparison of Variable Methods of Determining CMC

Variable methods have been proposed hitherto for CMC-determination, and it is convenient to classify them as follows. (Table 1) In the 2nd and 3rd column are expressed the possibilities of various methods to determine 1st and 2nd CMC respectively in which positive and negative use is expressed with ⊕ and ⊖. In the 4th column are tabulated the possibilities of giving the information concerning the shape of micelle. The 5th column shows the accuracy of the methods in which many ⊕ signs express higher accuracy. The 6th column shows the degree of the experimental difficulty of the method and also number of ⊕ signs corresponds to its degree. Moreover, methods are classified in (I) and (II) groups before the 1st column. To (I) belong the methods which cause the change of the state of micelle at the measurement and also the change of CMC. (Generally, CMC falls by adding other substances.) (II) contains methods which cause no changes relatively.

Investigating Table 1, it is clear that light scattering is the best, and spectral dye method is the simplest. 2nd CMC can be determined only by diffusion and X-ray method. Moreover, there are a few methods which give some information about the shape of micelle. From all view points, we could conclude that light scattering method is the best among many methods. But this method requires an especially precise experiment under troublesome conditions and is not easy to perform. After all, there is no method which gives 1st and 2nd CMC, shape of micelle and moreover is easy to perform. The new viscosity method which we propose, gives 1st and 2nd CMC and has the possibility of giving the information concerning size of micelle, if very high accuracy is not demanded. That is why we insist upon this new viscosity method as a practical and useful one. (Viscosity method in Table 1 is not ours but that of Hess and others.)

The Method of Determining 1st CMC from Viscosity

Hess, Philippoff and Kiessig were the first who found the method of determining CMC from

Table 1

Methods of Determining CMC

	Method	1st CMC	2nd CMC	Size & Shape of Micelle	Accuracy of Method	Difficulty of Method	Literature
(I)	Solubilization	+	−	−	++	++	(7)
	Spectral Dye	+	−	−	++	+	(4)
	Diffusion	+	+	+	+	+++	(8), (9), (10)
(II)	Osmotic Coefficient	+	−	−	+	++	(11)
	Conductivity	+	−	−	+	++	(12)
	Density	+	−	−	+	+	(9), (13)
	Viscosity	+	−	−	+	+	(2)
	Surface Tension	+	−	−	+	+	(14)
	Light Scattering	+	−	+	+++	+++	(15), (16)
	X-rays	−	+	+	+	+++	(2), (17)
	Membrane Potential	+	−	−	+	++	(18)
	Flow Birefringence	−	−	+	+	+++	(19)

(7) R. S. Stearns, H. Oppenheimer, E. Simon and W. D. Harkins, *J. Chem. Phys.*, **15**, 496 (1947).

(8) G. S. Hartley and D. F. Runnicles, *Proc. Roy. Soc.*, **A168**, 420 (1938).

(9) R. J. Vetter, *J. Phys. Colloid Chem.*, **51**, 262 (1947).

(10) H. Okuyama, S. Saito and K. Tyuzyo, presented at the 4th Year Meeting of the Chemical Society of Japan in Tokyo, 1952.

(11) J. W. McBain and A. P. Brady, *J. Am. Chem. Soc.*, **65**, 2072 (1943).

(12) J. W. McBain, Frontiers in Colloid Chemistry, p. 113 (1951).

(13) K. A. Wright and H. V. Tartar, *J. Am. Chem. Soc.*, **61**, 544 (1939).

(14) A. E. Alexander, *Trans. Faraday Soc.*, **38**, 248 (1942).

(15) P. Debye, *J. Phys. Colloid Chem.*, **53**, 1 (1949).

(16) P. Debye, Ann. N. Y. Acad. Sci., **51**, 575 (1949).

(17) R. W. Mattoon, R. S. Stearns and W. D. Harkins, *J. Chem. Phys.*, **16**, 644 (1948).

(18) C. W. Carr, W. F. Johnston and I. M. Kolthoff, *J. Phys. Colloid Chem.*, **51**, 636 (1947).

(19) H. A. Scheraga and J. K. Backus, *J. Am. Chem. Soc.*, **73**, 5103 (1951).

η_r (relative viscosity) or $1/[\eta]$ ($[\eta]$ is the solpe of η_r vs. C-curve.) We have already discovered that η_{sp}/C_m vs. concentration curve of Potassium-caprate becomes minimum at 1st CMC[19]. (η_{sp}: specific viscosity $=\eta_r-1$, C_m: soap conc. in mol./l.) Further examining the existing data, we found, almost without exceptions, the curve with one maximum and minimum as Fig. 1. Namely, η_{sp}/C_m becomes minimum at some value of C_m, i. e. C_{m1}, and C_{m1} value is somewhat lower than C'_{m1} which is obtained from the knick of η_r, in many cases. Moreover, η_{sp}/C_m becomes maximum in lower part of C_{m1} in many cases. As the examples, we show the data of Dodecylamine-hydrochloride at 20° and 30°C. in Fig. 2[20] and

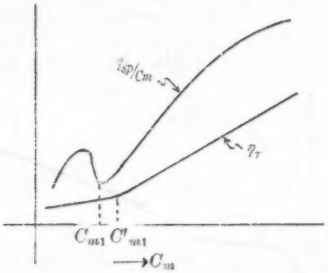

Fig. 1.

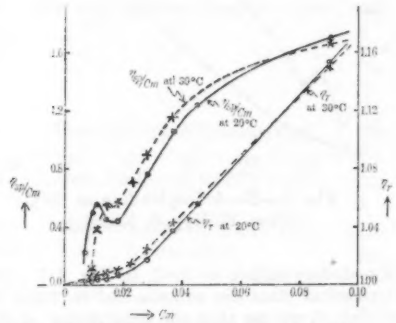

Fig. 2.—Dodecylamine-hydrochloride at 20 and 30°C. (K. Tyûzyô)

Table 2

1st CMC determined by the new Viscosity-Method

Substance	Temp. (°C)	1st CMC(A)	CMC from η_r	C_{m1}	Author	Literature
Na-caprylate	20	—	(0.36)	0.07(E)	Lamm, Högberg (1940)	(21)
Na-nonylate	20	0.22	0.22	0.24	Hess, Philippoff Kiessig (1939)	(2)
Na-caprate	20	0.10	0.12(B)	0.10(B)	Lamm, Högberg (1940)	(21)
K-caprate	20	0.10	0.08(C)	0.07(C)	Okuyama, Tyuzyo Saito (1951)	(10)
Na-laurate	20	0.025	0.096	0.031	Hess, Philippoff Kiessig (1939)	(2)
Dodecylamine-HCl	20	0.0132	0.023	0.015	Tyuzyo (1951)	(20)
	30	0.0132	0.020	0.016	Tyuzyo (1951)	(20)
Na-dodecyl-sulfate	40	0.010	0.012	0.012	Wright, Tartar (1939)	(13)
	70	0.012	0.017	0.014	Wright, Tartar (1939)	(13)
Na-oleate	20	0.001	0.23(D)	—(D)	Hess, Philippoff Kiessig (1939)	(2)
Hexanolamine-caprylate	20	—	0.35	0.26	Gonick (1946)	(22)
Aerosol-MA	25	—	0.029	0.027	Vetter (1947)	(9)

(A) 1st CMC in the 3rd column is the average value derived from the several different methods.

(B) Sodium-caprate has two minimum and the larger one coinsides with 1st CMC.

(C) In Potassium-caprate, CMC from η_r is closer to 0.10 than C_m, but in this case, 0.044 n KOH is added as the swamping electrolyte for diffusion and so CMC must somewhat fall. Therefore, the method of η_{sp}/C_m is not inferior than the one of η_r even in this case.

(D) 1st CMC of Sodium-oleate cannot be determined from viscosity method becaues its value (0.001) is too small. The value (0.23) of Hess and others is very large. Perhaps they mistook 2nd CMC for 1st CMC. (Also see Section 4.)

(E) C_{m1} of Sodium-carylate is too small contrary to expectation.

(F) Sodium-dodecylsulfate has no minimum at 50 and 60°C. It has only a knick at 70°C.

(G) Both Sodium-capronate and Sodium-valeriate have no minimum. It seems probable that there exist no micelles in the studied range of concentration.

(20) K. Tyuzyo, Unpublished.

(21) O. Lamm and H. Högberg, *Kolloid-Z.*, **91**, 10(1940).

(22) E. Gonick, *J. Am. Chem. Soc.*, **68**, 177 (1946).

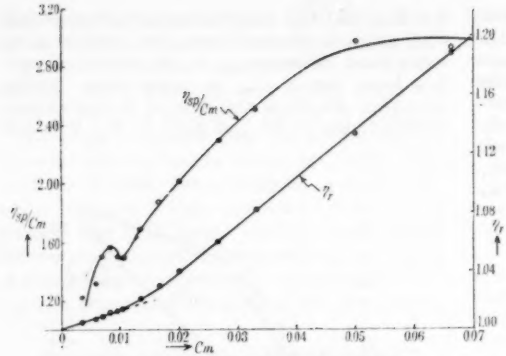

Fig. 3.—Na-dodecylsulfate at 20°C.
(Hess, Philippoff, Kiessig)

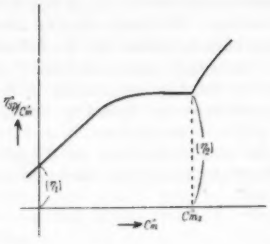

Fig. 4.

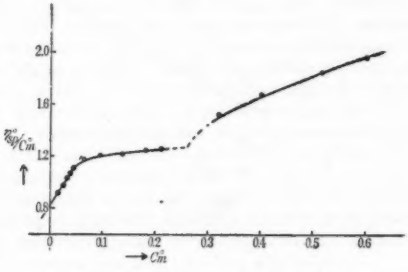

Fig.5.—Na-nonylate at 20°C.
(Hess, Philippoff, Kiessig)

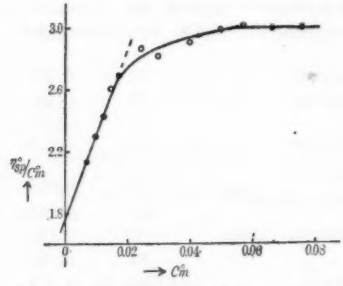

Fig. 6.—Na-dodecylsulfate at 20°C.
(Hess, Philippoff, Kiessig)

Sodium-dodecylsulfate at 20°C. in Fig. 3.[2] All the numerical data are summarized in Table 2. From Tab. 2, we see that the coincidence of C_{m1} and 1st CMC from other methods is satisfactory. Moreover, because C_{m1} corresponds to the distinct "minimum" of η_{sp}/C_m vs. C_m curve, it could be determined more accurately than the rather vague "knick" of η_r.

The Method of Determining 2nd CMC from Viscosity

2nd CMC is defined with the concentration where I-band in X-ray diffraction begins to appear,[17] but almost no other physico-chemical properties are investigated in such a region of high concentration. Only a few abnormalities were found in diffusion measurement.[9][10]

Now, we can presume that above 1st CMC, concentration of detergent monomer in solution which is in equilibrium with micelle is almost constant and unchanged.[16] Accordingly, we make the following operations.

$$C_m^\circ = C_m - C_{m1} \tag{1}$$

$$\eta_{sp}^\circ/C_m^\circ = (\eta_r^\circ - 1)/(C_m - C_{m1}) = (\eta_r/\eta_{r\min})^{-1}/(C_m - C_{m1}) \tag{2}$$

where,

C_m°: detergent concentration defined with equation (1)
C_m: detergent concentration in mol./l.
C_{m1}: 1st CMC derived from above viscosity method
$\eta_{r\min}$: relative viscosity of solution against water at 1st CMC

If we plot $\eta_{sp}^\circ/C_m^\circ$ against C_m°, we obtain the curve as Fig. 4 almost without exceptions.[23] As the examples, we have shown in Fig. 5 and Fig. 6 the results of sodium-nonylate and sodium-dodecylsulfate.[2] From the figures, we see that $\eta_{sp}^\circ/C_m^\circ$ increases linearly with C_m° as long as C_m° is small and thereafter passing a knick, converges to the constant value, i. e. $[\eta_2]$ in Fig. 4. Then the second and more sharp knick appears when C_m° reaches to some value, i. e. C_{m2}° from where $\eta_{sp}^\circ/C_m^\circ$ increases suddenly again. After all, $[\eta_1]$ and $[\eta_2]$ are defined with the following equations.

$$[\eta_1] = \lim_{C_m^\circ \to 0} (\eta_{sp}^\circ/C_m^\circ) \tag{3}$$

$$[\eta_2] = \lim_{C_m^\circ \to C_{m2}^\circ} (\eta_{sp}^\circ/C_m^\circ) \tag{4}$$

The meaning of $[\eta_1]$ and $[\eta_2]$ will be explained in the next section. Moreover, we have C_{m2} from the next equation.

(23) There are only few data on the viscosity measurement over the wide range of concentration, and so in some cases we connect two independent data.

Table 3

2nd CMC determined by the new Viscosity-Method

Substance	Temp. (°C.)	C_{m2}(*) in wt. %	2nd CMC in wt. %	Method of determining 2nd CMC	Author	Literature
Na-nonylate	20	9~10	—	—	—	—
K-caprate	—	—	22.9	X-rays	Mattoon, Stearns, Harkins (1948)	(17)
K-laurate	20	10.7~13.1	12.20	X-rays	〃 〃 〃	〃
K-myristate	20	8.0~10.7	7.16	X-rays	〃 〃 〃	〃
Na-palmitate	60	5.6~ 6.7	—	—	—	—
Na-stearate	60	3.1~ 3.7	—	—	—	—
Na-dodecyl-sulfate	40	6~9	4~5	X-rays	Hess, Philippoff Kiessig (1939)	(2)
	70	6~9				
Na-oleate	20	4.39	7.2	Viscosity	Hess, Philippoff Kiessig (1939)	(2)
			4~5	X-rays	〃 〃 〃	〃
			5~6	Diffusion	Okuyama, Tyuzyo, Saito (1951)	(10)
Aerosol-MA	25	2.99	4.5	Partial specific Volume	Vetter (1947)	(9)
			2.5	Diffusion	〃	〃

(*) In many cases, $\eta_{sp}^{\circ}/C_m^{\circ}$ vs. C_m° curve gives no sharp knick so that C_{m2} is expressed in an extended range and not a fixed value. For this fact, the method itself is not responsible but the insufficiency of the experimental data is the real reason.

$$C_{m2}=C_{m1}+C_{m2}^{\circ} \qquad (5)$$

In the Table. 3 are shown C_{m2}-values from above method and the existing values of 2nd CMC. It will be understood from the table that our C_{m2} values fairly coincide with 2nd CMC obtained from other methods. This method of determining 2nd CMC seems to be quite satisfactory at the present stage. (The data of X-rays are not quite accurate themselves.)

Table 4

Values of $[\eta_1]$ and $[\eta_2]$

Substance	M	Temp. (°C.)	$[\eta_1]$	$[\eta_2]$
Na-caprylate	166.21	20	0.65	0.87
Na-nonylate	180.23	20	0.81	1.28
Na-caprate	194.25	20	0.67	—
	〃	20	1.19	—
K-caprate	210.35	20	0.87	—
Na-laurate	222.30	20	1.18	(2.2)
K-laurate	238.40	20	—	2.6
K-myristate	266.48	20	—	3.3
Na-Palmitate	278.42	60	—	2.0
Na-stearate	306.48	60	—	2.5
Na-dodecylsulfate	302.37	20	1.78	3.0
		40	2.23	2.65
		70	1.94	2.57
Dodecylamine-HCl	221.80	20	0.88	2.0
		30	0.94	1.9
Na-oleate	304.34	20	1.35	—
		20	—	3.81
Aerosol-MA	388.46	25	1.73	1.84
Hexanolamine-caprylate	221.80	25	1.13	—

The Meaning of $[\eta_1]$ and $[\eta_2]$

We tabulate in Table. 4 $[\eta_1]$ and $[\eta_2]$ values obtained from above method. M in the second column of the table is the molecular weight of the detergent monomer. $[\eta_1]$ would be the related quantity to the micelle molecular weight (M_m) from the analogy of high polymer solutions. But unfortunately, M_m has hardly ever been measured accurately up to this time. And so it is impossible to compare $[\eta_1]$ with M_m directly. Therefore, for convenience, we plotted $[\eta_1]$ and $[\eta_2]$ against M (monomer molecular weight) in Fig. 7 and Fig. 8.

The following facts are recognizable from these figures.

(a) Fatty acid anionic soap series lie almost on the straight line.

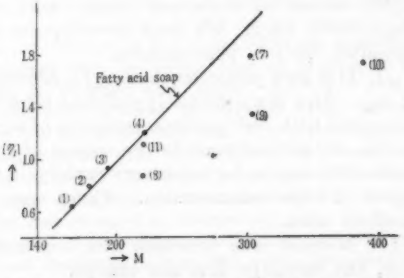

(1) Na-caprylate; (2) Na-nonylate; (3) Na-caprate; (4) Na-laurate; (5) K-laurate; (6) K-myristate; (7) Na-dodecyl-sulfate; (8) Dodecylamine-HCl; (9) Na-oleate; (10) Aerosol MA; (11) Hexanolamine-caprylate

Fig. 7.—Relation between $[\eta_1]$ and M.

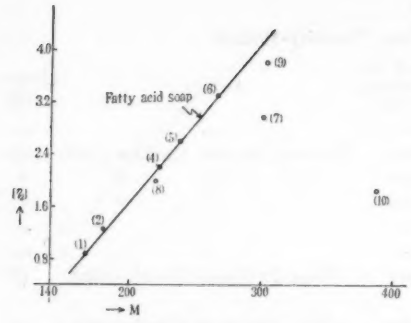

Fig. 8.—Relation between $[\eta_2]$ and M

(b) $[\eta_1]$ of sodium-oleate is exceptionally small, whereas its $[\eta_2]$ is not very small.

(c) $[\eta_1]$ and $[\eta_2]$ of sodium-dodecylsulfate are both abnormally small.

(d) $[\eta_1]$ of dodecylamine-hydrochloride is smaller than that of anionic soap, but $[\eta_2]$ is almost equal.

(e) $[\eta_1]$ and $[\eta_2]$ of aerosol-MA (sodium-methylamyl-sulfosuccinate) are both much smaller than those of ordinary fatty acid soap.

Discussion

(I) The phenomenon that η_{sp}/C_m becomes minimum at C_{m1} (Section 3) may probably be due to the result of the electrostatic interaction, owing to the strong electrolytic character of soap molecules. (η_{sp}/C_m of polyelectrolyte solutions passes generally a minimum value at some concentration.) However, most recently, R. Goto, N. Koizumi and T. Sugano found that η_{sp}/C_m of polyethleneoxide-monoalkylether solutions (nonionic detergent) also reaches a minimum in the neighbourhood of CMC.[24] Therefore, this phenomenon seems to be common to ionic and nonionic detergent which cannot be explained simply with the electrostatic force. We have no adequate explanation for this phenomenon.

(II) It is very particular that $\eta_{sp}^{\circ}/C_m^{\circ}$ converges to $[\eta_2]$. This is a completely different behavior compared with high polymer solutions of which η_{sp}/C_m is proportional to the square of concentration and so increases very rapidly in the region of high concentration. There seem to be three cases.

(i) Micellar size increases with concentration, but its shape does not change.

(ii) Shape changes with increasing concentration, whereas its size stays unchanged.

(iii) Size increases and shape also changes with increasing concentration.

Which of those three possibilities is most reasonable cannot still be decided. The recent investigation of flowbirefringence of detergent solutions[19] seems to be important in order to aquire some information of the micelle size and shape at moderately high concentration. At present, there is no direct means to determine both micellar size and shape simultaniously over wide range of concentration. Our discussion therefore is obliged to be limited to the indirect one. The most effective method, i. e. light scattering, can decide M_m only at low concentration and is not applicable at high concentration. Moreover, in the condition without adding electrolyte, it is impossible to dicide the micelle shape from the assymmetry of the scattered light, because micelle is too small in this condition. On the other hand, X-ray method gives some information of micelle size and shape at high concentration, but cannot be applied to low concentration. With diffusion method, it is necessary to add some swamping electrolyte in the soap solution, nevertheless micelle size is given only under some assumptions concerning hydration. At any rate, for detailed analysis of th above phenomena, many experimental data are still lacking.

(III) It must be remarked that $[\eta_1]$ and $[\eta_2]$ and M (monomer molecular weight) has a linear relation for fatty acid homologue. The fact that sodium-oleate dislocates the linearity could be explained from abnormal physical properties of oleic acid based on its cis-configuration. For example, it has abnormal low meltingpoint (14°C.) and high density (0.895). Aerosol-MA dislocates also, but it is natural if we remember that its micelle is quite different from ordinary soap because its monomer has the hydrophilic group nearly at the center. The difference between cationic and anionic soap micelles may be based upon the difference of the hydrophilic character of their hydrophilic group. The difference between sodiumdodecylsulfate and fatty acid soap is due also to the same cause. If M_m of several detergents are measured accurately by the light scattering, we can expect that the relation such as $[\eta_1]=KM_m^n$ may be concluded from those data.

Summary

(1) Several methods of determining CMC are compared and criticised.

(2) A new method of determining 1st CMC from viscosity is experimentally established.

(24) R. Goto, N. Koizumi and T. Sugano, presented at the 5th Annual Meeting of the Chemical Society of Japan in Tokyo, 1952.

(3) A new method of determining 2nd CMC from viscosity is established by transforming concentration and viscosity in the new variables.

(4) Of each soap, characteristic constants $[\eta_1]$ and $[\eta_2]$ are discovered, and it is shown that a definite relation is concluded between these values and monomer molecular weight.

(5) The theoretical explanation of these newly found phenomena has not yet been made.

Department of Chemistry, Faculty of Science, Osaka University, Osaka

---

New Spraying Reagents for the Detection of Reducing Sugars on the Paper Chromatograms

By Susumu HIRASE, Choji ARAKI and Susumu NAKANISHI*

(Received September 19, 1952)

Since paper chromatography was first applied to carbohydrates by Partridge,[1] various spraying reagents have been reported for the detection and identification of sugars separated on a paper chromatogram. Acidic solutions of aromatic amines such as aniline[2] and benzidine,[3] or of phenols such as resorcinol and naphthoresorcinol,[4] have been most frequently employed as spraying reagents. Their use depends upon the formation of furfural or its derivative by the action of an acid upon the sugar, and its subsequent condensation with an amine or phenol to give a colored compound. Among them, amine reagent is generally sensitive to aldoses, but is not so sensitive to ketoses and sometimes gives only faint spots. Whereas the sensitivity of phenol reagent to ketoses is excellent, its sensitivity to aldoses is moderately poor. Therefore, for complete detection of components in a mixture of unknown sugars by means of paper chromatography, such disadvantage has been experienced that both amine and phenol reagents must be applied.[5] If, however, aminophenols, carrying amino and phenolic hydroxyl groups, are used instead of an amine or phenol alone, they may be expected to be universal reagents in order to detect both aldoses and ketoses in one spraying operation. In this expectation, several aminophenols have been examined as the color reagents for reducing sugars, and an alcoholic solution of *o*-aminophenol acidified with phosphoric acid has been found to be the most useful one in respect of its universal sensitivity for various types of sugars and its specific coloration.

Experimental

Spraying Reagents: Of aminophenols were examined *o*-, *m*- and *p*-aminophenol, 1-amino-2-naphthol, 2,4-diaminophenol and 2-amino-resorcinol, the last two being used in the form of their hydrochlorides because of the unstability of their free bases. The reagent was prepared before use by dissolving 0.15 g. of each aminophenol in 20 cc. of ethanol and acidifying it with 10 cc. of 50% (w/w) phosphoric acid.

General Procedure: By means of micropipettes, the solutions of various concentrations of a sugar were spotted side by side at intervals of 2 cm. on a starting line of a filter paper sheet (Tōyō filter paper No. 2) so that each spot carried 1, 2, 3, 5, 10, 15 and 20 μg. of the sugar, respectively. The chromatogram was irrigated in the ascending technique with the upper layer of a mixture of butanol, ethanol and water (4:1:5 V/V), the solvent being allowed to advance about 30 cm. from the sugar starting line. The paper was then dried, sprayed with the reagent, and heated in an oven at 105° for a few minuites until a series of sugar spots with successively decreasing intensities was revealed in decreasing order of sugar quantity. The background of the paper remained almost unaffected. Thus, the minimum quantity of the sugar which was detected by each reagent was measured, and the color of the spots was also observed. Experiments were repeated several times for each L-arabinose, D-xylose, D-ribose, L-rhamnose, D-glucose, D-mannose, D-galactose, D-fructose, L-sorbose, D-tagatose, lactose, sucrose,

* Faculty of Engineering, Dōshisha University, Kyoto.

(1) S. M. Partridge *Nature*, **158**, 270 (1946).
(2) S. M. Partridge, ibid., **164**, 444 (1949).
(3) R. H. Horrocks, ibid., **164**, 443 (1949).
(4) W. G. C. Forsyth, ibid, **161**, 239 (1948).
(5) S. Hirase and C. Araki, *Memoirs of Faculty of Industrial Arts, Kyoto Technical University*, **1**, 19 (1952)

Table 1

The Observed Color and the Sensitivity (in μg. unit) of Each Sugar Class to Various Aminophenol Reagents

Sugar Classes	Aminophenols											
	o-Aminophenol		*m*-Aminophenol		*p*-Aminophenol		1-Amino-2-naphthol		2,4-Diaminophenol*		2-Aminoresorcinol*	
Pentose	Blue	1	Brown	2	Reddish brown	5	Blue	5	Dark blue	1	Blue	5
Methylpentose	Cherry red	5	Brown	5	Yellowish brown	5	Purple	15	Orange	5	Orange red	15
Aldohexose	Brown	5	Brown	5	Yellowish brown	5	Brown	15	Brown	5	Brown	15
Ketohexose	Lemon yellow	1	Lemon yellow	1	Lemon yellow	1	Lemon yellow	1	Lemon yellow	1	Lemon yellow	1
Lactose	Brown	5	Brown	5	Brown	5	Brown	15	Brown	5	Brown	15
Sucrose	Yellow	1	Yellow	1	Yellow	1	Yellow	1	Yellow	1	Yellow	1
Uronic acid	Blue	1	Reddish brown	1	Reddish brown	1	Blue	1	Blue	1	Blue	1

* u ed as its hydrochloride since its free base was unobtainable.

D-glucuronolactone, D-mannuronolactone and D-galacturonic acid. The results are summarized in the accompanying table.

Results

It will be seen from the table that all of the reagents are more or less effective to detect sugars, though the preliminary expectation is not completely satisfied. Generally speaking, they are particularly sensitive to ketoses and ketose-containing sucrose, giving a yellow color. Uronic acid or its lactone is also detectable with superior sensitivity. With regard to aldoses, pentose can be detected more sensitively than methylpentose and aldohexose, and gives the same coloration as that of uronic acid or its lactone.

Among these reagents, *o*-aminophenol reagent is found to be the most valuable one, for it detects as little as $1\sim5\,\mu$g. of each sugar and yields a specific color with each particular class of sugars. Although 2,4-diaminophenol reagent also seems to be possessed of these advantages, it is inferior to the former due to its unstability. With *o*-aminophenol reagent, it is easily achieved to decide the sugar class to which an unknown sample belongs, and, moreover, methyl glycosides give the same colorations as those of their parent sugars. For example, methyl xyloside and methyl glucoside give blue and brown color, respectively. Sugar alcohols are lacking in any coloration.

The authors wish to express their hearty thanks to Mr. K. Yamanouchi for his kind assistance in the course of this study.

Institute of Chemistry, Faculty of Industrial Arts, Kyoto Technical University, Kyoto

Studies on the Mechanism of the Electrolytic Formation of Perchlorate.* I.

By Kiichiro SUGINO and Shigeru AOYAGI

(Received November 17, 1952)

Introduction and Outline of the Research

Preparation of peracids is the typical electroprocess which can not practically succeed by any other method. Especially, the production of perchlorate or persulphate is one of the most important electrolytic processes now operated in the world.

Anodic potential of the formation of perchlorate has been considered to be very high and this electrolytic preparation has been successfully accomplished only by the use of smooth platinum anode which has the highest oxygen overvoltage. One of the authors has already developed a new electrolytic process of this production using lead peroxide anode instead of platinum. In this case, in order to increase the oxygen overvoltage of lead peroxide anode, a small amount of sodium fluoride must be added in the electrolyte. The reason for these devices is that even if the anodic potential of the formation of perchlorate is very high, it can not proceed unless at the lower potential than that of oxygen evolution. But the anodic potential of the formation of perchlorate has not yet been accurately determined and the variation of it with the concentration of chlorate has also remained unknown. Therefore, the present study seeks to measure the anodic potential of perchlorate formation accurately and at the same time to present the most probable mechanism of this anodic process.

Twenty five years ago, the polarographic method was proposed by Heylovský and Shikata and the electrolytic reduction potential of organic compounds which is lower than that of hydrogen evolution at the dropping mercury cathode and the variation of it with the concentration of the depolariser can now be measured very easily by that method. So the authors tried to apply the same method to the anodic process of peracid formation to determine the potential at which the reaction occurs. If the anodic potential of perchlorate formation is lower than that of oxygen evolution at platinum anode, a typical anodic polarogram will be obtained by a platinum micro-anode, just the same as the cathodic polarogram of the reduction process described above. The resulting polarogram assumed is shown in Fig. 1.

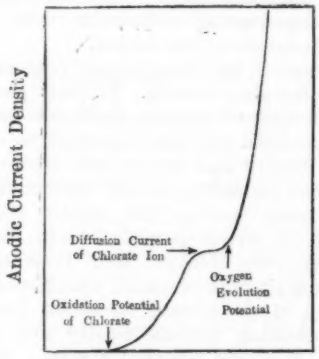

Fig. 1.

And the variation of the anodic potential with the concentration of chlorate will be approximately represented by the following formula.

$$E=\frac{RT}{2F}\ln\frac{K}{C_{ClO_3^-}\cdot a^2_{OH^-}}$$

where $C_{ClO_3^-}$ is the concentration of chlorate having a definite value and K is a constant. If these assumptions are verified by the experiments, the formation of perchlorate must be expressed by the following mechanism;[1]

$$2OH^- - 2e \rightarrow 2OH \rightarrow O + H_2O$$
$$ClO_3^- + O \rightarrow ClO_4^-$$

Upon these assumptions, the current-

* This papar was already given in the lecture at the general meetings of the Electrochem. Soc. of Japan held on May 1949, April 1950 and April, 1952.

(1) Bennett and Mack, *Trans. Electrochem. Soc.*, **29**, 323 (1916).

potential curves of the electrolytic oxidation of chlorate were measured polarographically under various conditions. The nature of the polarogram thus obtained was quite different from that of the usual oxidation-reduction process as shown in Fig. 1 and from the polarogram, it was pointed out that the anodic potential of the oxidation of chlorate might be higher than that of oxygen evolution. And even the phenomenon which was probably the limiting current of the discharge of OH^- ion could also be seen in the polarogram. These results were not able to be completely explained by the usual mechanism described above. In order to explain the results more suitably, the authors proposed an alternative mechanism, in which the discharge of chlorate ion and the subsequent combination and hydrolysis of ClO_3 were assumed.[2][3] This mechanism has already been proposed by other investigators, but no experimental verifications were found in the literature of the subject.

The research has been further continued to confirm the above results. For this purpose, the electrolysis of chlorate solution at definite anodic potential was carried out and the anodic current density and the current efficiency of perchlorate formation at that current density were plotted against the anodic potential applied. A current-potential curve like the polarogram was obtained from these experiments and it was observed that the current efficiency of perchlorate formation increased with increasing current density due to the increase of anodic potential applied. And in spite of no perchlorate formation in the electrolysis of a very dilute aqueous solution of chlorate, it was also observed that when the same amount of chlorate dissolved in a concentrated perchlorate solution was electrolysed (this is the case of practical perchlorate cell), perchlorate was formed in a fair current efficiency. In addition to this, perchlorate solution itself gave an analogous polarogram as chlorate in which the discharge potential of perchlorate ion was observed at higher value than that of oxygen evolution. From these experiments, it was made clear that the first step of perchlorate formation was probably the discharge of chlorate ion. And it may be supposed that the reason for the possibility of discharge of chlorate ion is not only the high oxygen overvoltage of special anodic materials, but also the lack of water in the neighbourhood of the electrode surface due to the extraordinarily high salt concentration of the electrolyte and also to the strong hydration power of existing ions. (The latter was verified by further experiment.) These results will be reported successively. In this paper, only results obtained from the measurement of anodic polarogram of the electrolysis of chlorate and a possible mechanism based upon the polarogram were given.

(Part I) Anodic polarogram of the Electrolysis of Chlorate by a Platinum Microanode

Measurement of Current-potential Curves

A micro-rotating platinum electrode and a smooth platinum plate of sufficiently large area were used as the anode and the cathode respectively. The details of the cell design and the measurement circuit are shown in Fig. 2-b and Fig. 2-a.

(1) **Electrolytic Cell.** — The section of the platinum wire of 0.3 mm. diameter sealed in a glass tube was used as the anode, the area of which was about 10^{-3}~10^{-4} cm^2. The cathode was a platinum plate of 10 cm^2. Throughout the following electrolysis, the current being less than 7×10^{-4} amp., the potential drop across the electrolyte did not amount to 10 mv. which was the limit of accuracy of our potential measurement. The stem of the anode—a glass tube—was rotated at 1000 r. p. m.. Although the significance of this rotation is not very important, it prevents the accumulation of oxygen gas on the surface of the anode and maintains the thickness of the anodic diffusion layer unchanged during the measurement and so a better reproducibility in the measured current-potential curves may be expected.

(2) **Polarograph.** — The sensitivity of the galvanometer used was 3.5×10^{-6} amp./mm./m..

(3) **Apparatus for the cathodic potential measurement.**—Since the cathode has a large area and the current is very small, the polarisation at cathode is generally considered to be very small. But in our case, it was found that it amounted to about 500 mv. for the cathodic current density of 3.5×10^{-3} amp./cm^2.. Thus, the cathodic potential must be measured continually throughout the current-potential curve measurement. For this purpose, the simple apparatus illustrated in Fig. 2-a was sufficient and also very convenient, the sensitivity of which was 3 mv., and the range of measurement, -450 mv.~$+450$ mv..

(4) **Temperature.** — The electrolytic cell and the calomel electrode were immersed in a thermostat regulated at $17°C\pm0.02°$.

(5) **Electrolyte.**—1~6 mol./l. aqueous solutions of sodium chlorate were used. It is seen that the use of such a high concentration of the

(2) Oschsli, *Z. Electrochem.* **9**, 807 (1903).
(3) Knibbs and Palfreeman, *Trans. Faraday Soc.*, **16**, 402 (1920).

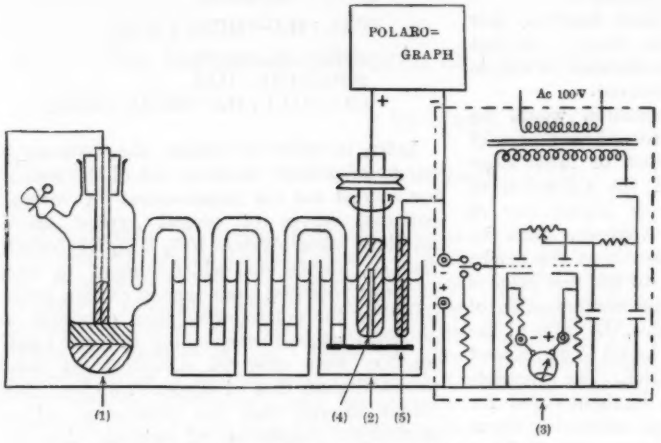

Eig. 2 a.—(1) Calomel Electrode (Saturated KCl Type)
(2) Electrolytic Cell, (3) Valve Voltmeter,
(4) Anode. (5) Cathode.

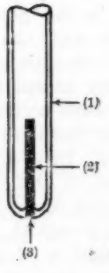

Fig. 2 b.—(1) Glass Tube
(2) Platinum Wire
(3) Anode Surface

electrolyte, together with the relatively large anodic current density mentioned above, makes the condition of our current-potential curve measurement deviate from that of the ideal polarographic method. But it was confirmed that for wellknown anodic processes (which occur at lower potential than that of oxygen evolution), usual polarograms were always given by the use of the same apparatus and under the same measuring conditions as described later.

Results and Discussion

The polarograms for various concentrations of sodium chlorate solutions are shown in Fig. 3. The abscissa corresponds to the anodic potential (the numerical values of which were obtained by subtracting the cathodic potential from the cell voltage and by referring to the hydrogen scale). The ordinate corresponds to the apparent anodic current density in amperes per dm^2. Its value, however, was not so reliable in consequence of the obscurity of the true apparent area of the anode.

The potentials of the second stage were seen to be:

about	2.1 V	for	5.6 M	solution
	2.1 〃	〃	4.0	〃
	2.2 〃	〃	2.8	〃
	2.4 〃	〃	2.0	〃
	2.4 〃	〃	1.4	〃

Some characteristics of the polarograms obtained may be summarized as follows:

(1) In a moderately concentrated solution of chlorate, two stages of potential were definitely observed, as shown in Fig. 3.

(2) In the first or lower stage, the potential has a value of about 1.7—1.9 v. On the other hand, in the second or higher stage, the potential has a higher value than 2.3 v.

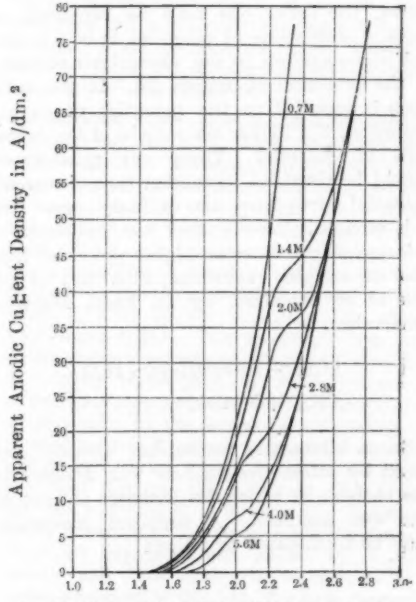

Fig. 3.

(3) Contrary to the usual polarogram, the height of the wave of the first potential stage was seen to be reversely proportional to the concentration of chlorate. It lowered as the

concentration of chlorate increased.

(4) For a sufficiently dilute solution, this wave height grew so high that it reached beyond the range of the measurement, a simple exponential curve being observed.

If an analogous interpretation would be made for our polarogram to ordinary ones of the cathodic process, the first or lower stage should be the potential of the oxidation of chlorate and the second or higher one of oxygen evolution. This, however, must be decidedly denied by the fact that the height of the wave corresponding to the first stage is reversely proportional to the concentration of chlorate. In addition to this, the value of the potential of first stage was found to correspond to the one of oxygen evolution. (The reversible oxygen potential, E_{O_2/OH^-}, is about 0.8 v. for any solution of pH 7 and estimating about 1v. of oxygen overvoltage of a smooth polainum plate at the current density of 1 amp./dm^2., the actual oxygen evolution potential for any solution concerned amounts to about 1.8 v.) So, among two potential stages mentioned above, the lower one may be supposed, on account of its value of potential, to be a potential corresponding to the electrolysis of water or the evolution of oxygen gas. If the lower stage is regarded as the potential of oxygen evolution, the higher one may be of the oxidation of chlorate. Thus, our polarograms should be classified in another type of current-potential curve from the ordinary one. And it is obviously certain that the oxidation of chlorate occurs at some higher potential than that of oxygen evolution. This fact is not able to be explained by an usual following mechanism.

$$2OH^- - 2e \rightarrow 2OH \rightarrow O + H_2O$$
$$ClO_3^- + O \rightarrow ClO_4^-$$

So an alternative mechanism already proposed by other investigators was adopted by the authors in which the discharge of chlorate ion was assumed. A supposed mechanism may be formulated as follows

$$2ClO_3^- - 2e \rightarrow 2ClO_3$$
$$2ClO_3 + H_2O \rightarrow HClO_3 + HClO_4$$

$$\left.\begin{array}{l} 2ClO_3^- - 2e \rightarrow 2ClO_3 \\ 2ClO_3 \rightarrow ClO_3 - O_3Cl \\ ClO_3 - O_3Cl + H_2O \rightarrow HClO_3 + HClO_4 \end{array}\right\} \quad (2)$$

Later, in order to confirm the accuracy of our polarographic method, one of the authors has carried out the measurement of current-potential curves of several typical anodic reactions (electrolysis of KCl, KBr, KI, $NaNO_2$, $Na_2S_2O_3$, Na_2SO_3 etc.) which seemed to occur at lower potential than that of oxygen evolution. In the polarograms thus obtained, the potential stages corresponding to each anodic reaction were observed definitely at lower potential than that of oxygen evolution. These results showed that the polarogram of the electrolytic oxidation of chlorate described above and the proposed mechanism based on the polarogram were both probably correct.

Further, in view of the prospective discussion of the dependence of the discharge of chlorate ion on the mechanism of perchlorate formation, it is necessary to know the true formation of perchlorate at the potential of second stage in Fig. 3. For this purpose, in the following research, the electrolysis of chlorate solution was carried out at a definite anodic potential, corresponding to the second stage in Fig. 3. under various conditions. Many interesting phenomena were observed and from the results obtained, our conclusion based upon the polarogram was seen to increase its appropriateness. These results will be reported hereafter.

The cost of this research has been mainly defrayed from the Grant in Aid for Fundamental Scientific Research of the Ministry of Education to which the authors' thanks are due.

Laboratory of Organic Electrochemistry and Biochemistry, Tokyo Institute of Technology, Tokyo

The Oxygen Equilibrium of Hemerythrin and Bohr Effect

By Masaji KUBO

(Received October 15, 1952)

The transfer of oxygen from the external environment into the tissues of various animals is accomplished by respiratory pigments capable of combining with oxygen when its partial pressure is high and of giving it up when the pressure is low. There are four different types of the pigments, hemoglobin, chlorocruorin, hemerythrin and hemocyanin. The first three contain iron while hemocyanin is a copper compound. Surely hemoglobin has been studied in the most extensive way.(1) Among the iron-containing respiratory pigments, hemerythrin is interesting in view of the fact that although the common property as an oxygen transporter confers upon all these types of molecules their biological analogy, the chemical properties of hemerythrin are very markedly different from those of hemoglobin and chlorocruorin. Oxygen combines with hemoglobin(2) or chlorocruorin(3) in definite proportion of one molecule per one atom of iron, whereas the gas combines with hemerythrin(4) in the proportion of one molecule per three atoms of iron in the pigment molecule. Besides hemerythrin is not a heme derivative as are hemoglobin and chlorocruorin.(2)(5) The oxygen dissociation curve of hemerythrin from sipunculus under physiological conditions has already been studied by Florkin.(2) The present investigation was undertaken in order to examine more closely the oxygen equilibrium and Bohr effect, which together with magnetic studies to be reported later will reveal some features of interest concerning the function of iron atoms in the molecule.

Preparation of Hemerythrin Solution.—The coelomic fluid of a species of sipunculid worm called phascolosoma from the Marine Biological Laboratory in Woods Hole was centrifuged to throw down the dark red violet corpuscles. The sediment was washed several times with 2.5% sodium chloride solution to remove the plasma completely. It was made up to 60% of the original volume with distilled water and left to stand in an icebox for about two hours to lake the corpuscles. The stroma was removed by centrifuging and the dark red violet solution after filtration through a hard filter paper was ready for use. The solution contained a minute amount of sodium chloride originating from the washing solution. This does not affect the results at all. The exact control of the concentration was unnecessary in the present experiment. Still the difference between the optical densities of reduced and oxygenated solutions gives an accurate relative concentration for each solution. The simultaneous determination of optical density difference and iron content for one solution to be reported in the following paper can convert the relative value to the absolute concentration in gram atoms of iron per cc.

Apparatus.—The apparatus used was essentially the same as that used in the earlier experiments(1) on hemoglobin. The spectrophotometric method was employed for the determination of the degree of oxygenation of hemerythrin. As a constant light source a 6 V., 30 W. microscope lamp was used. It was run from two heavy duty accumulators connected in parallel. The light was filtered through an interference filter backed by a blue masking filter to get monochromatic light of wavelength 4760 A. This wavelength was chosen as satisfying the basic requirement that it should be readily transmitted by both reduced and oxygenated hemerythrin solution, although much more readily by the former than the latter. The monochromatic light was then passed through an optical cell having a path length of 2.5 mm. for the light through the solution. Only 1 cc. of solution was enough to fill the cell. The cell was really a part of a tonometer made of glass, which could be evacuated and sealed by a rubber vaccine cap. The total volume enclosed in the vessel amounted to 292.5 cc. The light transmitted by the cell fell on a photomultiplier tube RCA 931. The current thus produced was passed through a suitably chosen high grade resistor and the resulting voltage drop was measured by means of a potentiometer with a Millivac vacuum tube millivoltmeter as a detector of the balancing point.

Experimental Procedure

The tonometer containing the oxygenated

(1) D. W. Allen, K. F. Guthe and J. Wyman, *J. Biol. Chem.*, **187**, 393 (1950).
(2) R. A. Peters, *J. Physiol.*, **44**, 131 (1912).
(3) H. M. Fox, *Proc. Roy. Soc. London*, B **115**, 368 (1934).
(4) M. Florkin, *Arch. intern. physiol.*, **36**, 247 (1933).
(5) R. Kobert, *Arch. ges. Physiol.*, **98**, 411 (1903) : G. F. Marrian, *Brit. J. Exptl. Biol.*, **4**, 357 (1927).

hemerythrin solution was evacuated and equilibrated three times with the atmosphere of 99.9% pure commercial nitrogen saturated with water, until the dark red violet solution changed into a pale milky white, almost colorless solution of reduced hemerythrin. The measurement of optical density of the medium was made putting the tonometer in the optical system. Then a desired amount of air was introduced into the tonometer through the vaccine cap by means of a syringe and hypodermic needle, calibrated as to the volume of delivery. The resulting oxygen pressure in the tonometer could be calculated from the volume of air introduced, that of the gas phase in the tonometer and the known composition of air, with due correction for the humidity of air. The correction was also made for the amount of oxygen taken up by the solution. It could be calculated from the volume of the solution, the concentration in gram atoms of iron per cc., and the percentage saturation of the hemerythrin with oxygen as given by the photometric measurements to be described in the following paragraph. This correction was usually small, amounting to less than a few per cent of the calculated pressure of oxygen. After the measurement of optical density of the solution at 20°C. for twelve different oxygen pressure was over, the last measurement was made on essentially 100 per cent oxygenated hemerythrin obtained by exposing the solution to atomospheric air. Because hemerythrin has high oxygen affinity, it was unneccessary to use pure oxygen at this point. The degree of saturation Y with oxygen of the hemerythrin solution was calculated as

$$Y=\frac{D-D_{\mathrm{red}}}{D_{\mathrm{ox}}-D_{\mathrm{red}}} \qquad (1)$$

where D's denote optical densities of the solution in equilibrium with oxygen of partial pressure p, completely deoxygenated and oxygenated solutions respectively. Since we were interested only in the difference of optical densities, it was convenient to use a neutral filter made of a piece of photographic film of appropriate darkness to reduce the value of I_0, the intensity of incident light, so as to make it match that of I, the intensity of light emerging from the cell. It should be noted that no knowledge of the extinction coefficients and the exact concentration was required for the calculation of Y values.

The prime requirement in this kind of experiment was accuracy as well as speed, since proteins are known to be subject to denaturation especially in solutions of pH values far apart from that of physiological condition. The agreement of individual data of I/I_0 was within 1%. The difference between the optical densities of reduced and oxygenated solutions amounted to about 1.3. Hence the probable error in the degree of saturation is estimated to be less than 1%. The crucial point seemed to lie not in physico-chemical measurement but rather in the biochemical problem of how to prepare definite specimens and how to minimize the effect of denaturation. The whole physico-chemical measurement comprizing twelve different values of oxygen pressure could be carried out in six hours. Thus a fresh sample could always be prepared on the day of measurement and used.

Results and Discussion

The first two experiments were made on unbuffered hemerythrin solutions of concentration 5.16 and 6.31×10^{-6} gram atoms of iron per cc. respectively. The pH value of the solution in oxygenated state as measured by a glass electrode was 6.25 pretty close to the isoelectric point 5.85.[6] The unbuffered solution was fairly stable and a solution left overnight in an icebox gave results practically identical with those of a fresher sample.

The degree of partial saturation Y with oxygen is plotted as a function of $\log p$, the logarithm of oxygen pressure in mm. Hg., in

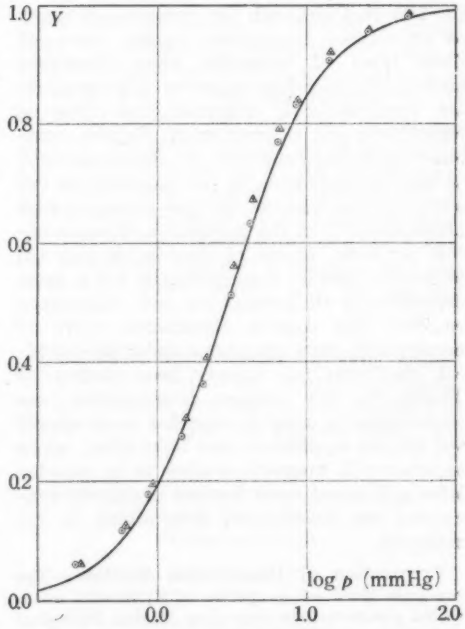

Fig. 1.—The degree of saturation with oxygen of hemerythrin as a function of the logarithm of the partial pressure of oxygen. 20°C., unbuffered, pH = 6.25. The circular points represent data on the solution of iron concentration 5.16×10^{-6} g. atom/cc., and the triangular points those of 6.31×10^{-6}. The full line depicts the empirical formula (2).

(5) J. Roche, *Ann. Rev. Biochem.*, **5**, 453 (1936).

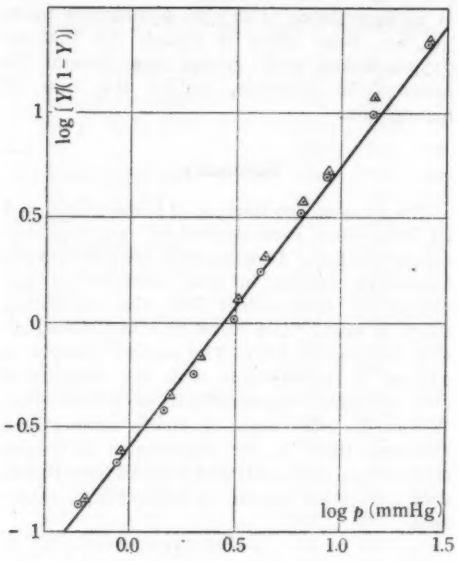

Fig. 2.—The dependence of $\log [y/(1-y)]$ upon $\log p$.

Fig. 1. The functional relation between Y and $\log p$ can be represented by the following empirical formula.

$$Y=\frac{1}{2}+\frac{1}{2}\tanh\left(2.303\frac{n}{2}\log\frac{p}{p_{1/2}}\right) \qquad (2)$$

with $n=1.37\pm.05$ and $\log p_{1/2}=0.46\pm.02$. This is mathematically equivalent to the statement that $\log [Y/(1-Y)]$ is a linear function of $\log p$,

$$\log\frac{Y}{1-Y}=n(\log p-\log p_{1/2}) \qquad (3)$$

as shown in Fig. 2. In fact the values of n and $\log p_{1/2}$ mentioned above were obtained in this way. From the equation (2) it is clear that $p_{1/2}$ is nothing but the partial pressure of oxygen in equilibrium with the solution in which the amount of oxygenated hemerythrin is just the same as that of the reduced form. The interpretation of the physical meaning of n in terms of the theory of linked groups is given in a paper by Wyman.[7] It will be found that the equation (3) can be written in an alternative way as follows.

$$\frac{Y}{1-Y}=\left(\frac{p}{p_{1/2}}\right)^n=Kp^n \qquad (4)$$

or Hill's empirical equation:

$$Y=\frac{Kp^n}{1+Kp^n} \qquad (5)$$

The constant K in the equation (4) may be interpreted, formally at least, as the equilibrium constant for the hypothetical reaction:

$$M+nX=MX_n \qquad (6)$$

$n=1$ would mean that all the oxygen attaching centers in the molecule are mutually independent, whereas $n=2$ that two centers are linked together so that an oxygen molecule attached to one center induces another oxygen molecule to combine with the molecule at once. The value $n=1.37$ in this case suggests that the oxygen combining centers in hemerythrin molecule are not completely independent, but the stabilizing interaction is weak, weaker at least than in the case of hemoglobin, in which case n was found to be 2.8.[7] This conclusion will be important in the interpretation of magnetic susceptibility of hemerythrin.

$\log p_{1/2}=0.46$ gives $p_{1/2}=2.9$ mm. Hg. Florkin[8] studied the oxygen dissociation curve of hemerythrin from sipunculus, and found for $p_{1/2}$ the value of 8 mm. Hg. at 19°C. It is doubtful that the disagreement is really significant in view of the fact that these samples were extracted from different animals and that the conditions were slightly different.

Finally the curve of Fig. 1 has a very slight but unmistakable asymmetry which cannot be ascribed to experimental errors. Wyman and others[7] found that the similar asymmetry in the case of hemoglobin disappeared for a freshly prepared material. In the present case even freshly prepared solution gave slight asymmetry of the curve and a material left to stand overnight revealed no sign of increased asymmetry.

Bohr Effect.—Further studies were made on the effect of pH on the oxygen equilibrium of hemerythrin. The measurements were made on solutions at 20°C. prepared in the same way as before, buffered with mixtures given in Table 1 chosen to get desired pH values, which were actually measured by a glass electrode. The oxygen equilibrium curves obtained were very similar to that of the unbuffered solution, except the case for pH=4.4, in which case though the curve was symmetrical it was less steep. The values of n and $\log p_{1/2}$ are summarized in Table 2. In the case of pH=4.4, slight denaturation was

(7) J. Wyman, *Adv. Protein Chem.*, **4**, 407 (1948).

(8) M. Florkin, *C. R. Acad. Sci.*, **195**, 832 (1932).

Table 1

Concentration of Hemerythrin (g. atom Fe/cc.)	Buffer Solution	Buffer Concentration	pH Value
4.95×10^{-6}	Na_2HPO_4-citric acid	0.035 M	4.4
5.16, 6.31	Unbuffered	—	6.25
4.10	K_2HPO_4-KH_2PO_4	0.095	6.8
5.55	Borax-boric acid	0.022	8.8

Table 2

pH	n	$\log p_{1/2}$
4.4	1.11±.05	0.57±.02
6.26	1.37±.05	0.45±.02
6.8	1.35±.05	0.44±.02
8.8	1.27±.05	0.46±.02

clearly perceptible by the appearance of fine pale yellow suspensions, and at pH=2.7 or 10.0 denaturation was so rapid that measurement could not be made at all. If progressive denaturation takes place, the decrease of concentration decreases D_{ox} in the equation (1) and results in the overestimation of Y in the lower left branch of the curve in Fig. 1, while in the upper right branch the simultaneous decrease of D and D_{ox} gives rise to the underestimation of Y, with the consequent flattening of the sigmoid curve. Taking this into account, we can conclude that within the pH range of stable hemerythrin solution there is no dependence of oxygen equilibrium upon pH, i.e., Bohr effect is absent. So that no oxygen-linked acid groups are present in hemerythrin molecule, unlike the case of hemoglobin.

Summary

The oxygen equilibrium of hemerythrin and its Bohr effect were studied by spectrophotometric method. It was found that the oxygen combining centers in this molecule are not completely independent but the stabilizing effect is weak. The value of n in Hill's equation is equal to 1.37. The partial pressure of oxygen in equilibrium with the solution of 50% saturated hemerythrin is 2.9 mm. Hg. Within the pH range of stable hemerythrin solution, there is no dependence of oxygen equilibrium upon pH, hence no oxygen-linked acid groups are present in hemerythrin molecule.

The present experiments were made at the Biological Laboratories, Harvard University. I wish to express my sincere thanks to Professor Jeffries Wyman, Jr. for his kind suggestions and advices.

Chemical Department, Faculty of Science, Nagoya University, Nagoya

---

Dipole Moments of Methyltropolones and their Bromoderivatives*

By Yukio KURITA, Toshikuni MIZUNO, Toshio MUKAI and Masaji KUBO

(Received November 19, 1952)

Proceeding with our work on the dipole moments of tropolone and its derivatives,[1] we made experiments on three methyltropolones and seven of their bromoderivatives. They were synthesized by one of us[2] and his collaborators. The position of substituents, which had already been inferred from evidences in organic syntheses,[2] could be confirmed by this physico-chemical method.

Experimental Results.—The apparatus and the method of measurement are already given in our previous paper.[1] The results are shown in Tables 1 and 2. The only datum found in literature to be compared with the present results is that of the compound II measured by Tyrell and Mills.[3]

* Read before the scientific meeting of the Chemical Society of Japan held on April 4, 1952.

(1) Y. Kurita, T. Nozoe and M. Kubo, *Bull. Chem. Soc. Japan*, **24**, 10, 99 (1951).

(2) T. Nozoe, T. Mukai, M. Kunori, T. Muroi and K. Matsui, *Sci. Reports Tohoku Univ.*, 1, **35**, 242 (1952).

(3) R. D. Haworth and J. D. Hobson, *J. Chem. Soc.*, **1931**, 561.

Table 1

Dielectric constant and density increments

	Compounds	w $\times 10^5$	$\Delta\varepsilon$ $\times 10^4$	Δd $\times 10^5$
I	Methyltropolone	192	192	47
	m. p. 50.5—51°	360	346	88
	25°	542	497	139
II	Methyltropolone	336	418	83
	m. p. 74—76°	598	728	141
	30°	940	1143	217
III	Methyltropolone	150	211	36
	m. p. 108—110°	331	422	75
	25°	512	663	123
IV	Bromomethyltropolone	321	267	128
	m. p. 123°	595	445	158
	25.6°	1086	899	458
V	Bromomethyltropolone	227	230	114
	m. p. 83—85°	514	507	215
	25°	674	677	282
VI	Bromomethyltropolone	230	80	138
	m. p. 171—172.5°	334	129	161
	25°	549	191	209
VII	Dibromomethyltropolone	271	158	123
	m. p. 140°	532	324	257
	30°	834	524	410
VIII	Tribromomethyltropolone	265	82	140
	m. p. 99.5—100.5°	588	176	309
	25°	766	225	421
IX	Bromomethyltropolone	213	194	94
	m. p. 115°	412	355	183
	30°	545	515	216
X	Dibromomethyltropolone	205	139	104
	m. p. 140°	404	283	202
	30°	630	404	321

Table 2

Dipole moments of methyltropolones and their derivatives

	t(°C.)	ε_1	d_1(g./cc.)	α	β(g./cc.)	$P_{2\infty}$(cc.)	R_D(cc.)	μ(D)
I	25	2.2753	0.87129	8.69	0.263	255.5± 1.0	37.1	3.27±.01
II	30	2.2637	0.86637	12.02	0.222	340.9± 1.6	37.1	3.88±.01
III	25	2.2744	0.87132	12.48	0.240	354.0± 8.2	37.1	3.94±.05
IV	25.6	2.2693	0.87036	8.38	0.455	375.9±20.6	44.8	4.05±.13
V	25	2.2727	0.87163	9.94	0.373	445.2± 8.2	44.8	4.42±.05
VI	25	2.2732	0.87221	3.39	0.224	192.0±13.6	44.8	2.68±.12
VII	30	2.2605	0.86614	6.51	0.310	406.6± 3.2	52.6	4.19±.02
VIII	25	2.2732	0.87124	2.86	0.554	247.6± 5.2	60.4	3.02±.04
IX	30	2.2608	0.86648	9.54	0.372	453.8±34.4	44.8	4.51±.19
X	30	2.2644	0.86627	6.22	0.509	389.5±21.2	52.6	4.27±.13

Their value of 3.9 D is in good agreement with ours.

Discussion.—The theoretical values for the moments of these compounds with substituents at various presumed positions were calculated as in our previous reports. The bond moment of methyl group substituted in tropolone was assumed to be equal to that in toluene; μ(C-CH_3) $=-0.4$ D. The calculated values are compared with the experiment in Table 3. We could thus determine definitely the position of substituents for all the compounds studied, except the compound V, for which we wish to defer our final decision.

Table 3

The position of substituents in methyl tropolones and their derivatives

Compounds	μ_{obs}(D)	μ_{calc}(D)	The position of substituents
I	3.27	3.41	3-Methyltropolone
II	3.88	3.76	4-Methyltropolone
III	3.94	3.90	5-Methyltropolone
IV	4.05	4.17	7-Bromo-3-methyltropolone
		1.95	5-Bromo-3-methyltropolone
V	4.42	4.24	3-Bromo-4-methyltropolone
		4.45	7-Bromo-4-methyltropolone
VI	2.68	2.27	5-Bromo-4-methyltropolone
		2.82	3,5-Dibromo-4-methyltropolone
		3.13	5,7-Dibromo-4-methyltropolone
VII	4.19	4.42	3,7-Dibromo-4-methyltropolone
VIII	3.02	2.93	3,5,7-Tribromo-4-methyltropolone
IX	4.51	4.48	3-Bromo-5-methyltropolone
X	4.27	4.56	3,7-Dibromo-5-methyltropolone

Summary

The dipole moments of three methyltropolones and their bromoderivatives were measured in benzene solution at 25° or 30°. The values obtained were compared with the theoretical data for the moments of these compounds with substituents at various presumed positions.

The final decision of the position of substituents were made as shown in Table 3.

We wish to express our thanks to Prof. T. Nozoe of Tohoku University for his kind suggestions and encouragement. Our thanks are also due to the Ministry of Education for aid in this research.

Chemical Institute, Faculty of Science, Nagoya University, Nagoya
Chemical Institute, Faculty of Science, Tohoku University, Sendai

---

Studies on Pyrethrins
The Synthesis of Some β-Keto Esters

By Masanao MATSUI, Tokuji YAMAGUCHI, Takeaki KATO and Giichi FUNAZO

(Received June 16, 1951)

Several methods are reported to prepare β-keto-esters through the condensation of methyl ketones and ethyl carbonate. The typical methods are those which use, as condensation agent, sodium alcoholate,[1] sodamide[2] and more recently sodium hydride.[3] Though the reaction yields depend upon the character of methyl ketones which are used, the best results can generally be obtained by employing sodium hydride, and the next best by sodium alcoholate. The sodamide method yields usually poor results, but is exempted from inconveniences which accompany the former two methods such as the work in the stream of nitrogen gas or the stirring under reduced pressure and the use of large excess of diethyl carbonate.

We, therefore, investigated the method to increase the condensation yield in the reaction by sodamide. We performed the reaction and found that the low yield of the reaction is due to the formation of urethan by a side reaction of this condensation.

A mechanism of this condensation proposed by Levine[2] is as follows;

$$(\mathrm{I})\quad CH_3COR+NaNH_2 \longrightarrow (CH_2COR)^-Na^+ + NH_3$$

$$(\mathrm{II})\quad C_2H_5OCO_2C_2H_5+(CH_2COR)^-Na^+ \longrightarrow RCOCH_2COOC_2H_5+NaOC_2H_5$$

$$(\mathrm{III})\quad RCOCH_2CO_2C_2H_5+(CH_2COR)^-Na^+ \longrightarrow (RCOCHCOOC_2H_5)^-Na^+ + CH_3COR$$

or

$$RCOCH_2CO_2C_2H_5+NaNH_2 \longrightarrow (RCOCHCOOC_2H_5)^-Na^+ + NH_3$$

The equations are correct as far as the mechanism is concerned, but the following side reactions also occur in reality. A part of ammonia produced in (I) and (III) reacts with diethyl carbonate and yields urethan and alcohol when two molecules of sodamide are used for one molecule of methyl ketones

$$(\mathrm{IV})\quad C_2H_5OCO_2C_2H_5+NH_3 \longrightarrow NH_2CO_2C_2H_5+C_2H_5OH$$

and the alcohol which is produced reacts with sodium enolate of the methyl ketone or with sodamide to produce ammonia.

$$(\mathrm{V})\quad C_2H_5OH+(CH_2COR)^-Na^+ \longrightarrow CH_3COR+C_2H_5ONa$$

or

$$C_2H_5OH+NaNH_2 \longrightarrow C_2H_5ONa+NH_3$$

The methyl ketone liberated by this reaction reacts sodamide and liberates ammonia, and ammonia repeats the reactions already described though ammonia decreases gradually by escaping from the reaction system. Thus we found that in order to minimize the reaction between ammonia and diethyl carbonate, it is necessary to produce sodium enolate of the methyl ketone at first, and in order to complete enolization of the methyl ketone or to complete the production of keto ester as far as possible, it is also necessary to employ more than two molecules of sodamide and more than one molecule, or probably more than two molecules, of diethyl carbonate to one molecule of the methyl ketone.

By using a methyl ketone, sodamide and diethyl carbonate in the molar ratio of 1:3:3 in the procedure described in the experimental part, we succeeded in obtaining almost the same yields of β-keto ester (See Table 1) as in the case of sodium hydride when the methyl

(1) Wallingford et al., *J. Am. Chem. Soc.*, **63**, 2252 (1941).
(2) R. Levine and C. R. Hauser, *J. Am. Chem. Soc.*, **66**, 1768 (1944).
(3) S. B. Soloway and F. B. LaForge, *J. Am. Chem. Soc.*, **69**, 2677 (1947).

Table 1

ketones	products	b. p.	n_D (temp., °C.)	yield % NaOCH$_3$ method	yield % old NaNH$_2$ method	yield % NaH method	yield % the present method	Analytical Data % Found	Analytical Data % Calcd.
Methyl ethyl ketone	Ethyl 3-oxo-valerate	91—93°/ 17 mm	1.4183 (23°)		13[2]		11	C 57.62 H 7.83	C 58.33 H 8.33
Methyl n-propyl ketone	Ethyl-3-oxo-caproate	93–95.5°/ 15 mm	1.4240 (30°)		19[2]		48	OC_2H_5 28.6	OC_2H_5 28.2
Allyl-acetone	Ethyl 3-oxo-6-heptenoate	95–100°/ 11 mm	1.4414 (22°)	70[4]		77[4]	70	OC_2H_5 25.8	OC_2H_5 26.5
Methallyl-acetone	Ethyl 3-oxo-6-methyl-6-heptenoate	105–115°/ 12.5 mm	1.4493 (15°)			70[4]	70	C 64.87 H 8.65	C 65.21 H 8.70
5-Hepten-2-one	Ethyl 3-oxo-6-octenoate	90–104°/ 7 mm	1.4397 (30°)			85[5]	69.5	OC_2H_5 25.0	OC_2H_5 24.4
6-Hepten-2-one	Ethyl 3-oxo-7-octenoate	102–120°/ 9.5 mm	1.4384 (30°)				75.5	OC_2H_5 24.9	OC_2H_5 24.4
Piperonyl-acetone	Ethyl 3-oxo-5-(3,4-methylene-dioxyphenyl)-valerate	160–163°/ 3 mm	1.5111 (30°)				32	C 63.32 H 6.10	C 63.63 H 6.07
Furfuryl-acetone	Ethyl 3-oxo-5-furylvalerate	110–120°/ 3 mm	1.4758 (16°)				22	C 64.78 H 7.05	C 62.86 H 6.67
Benzyl-acetone	Ethyl 3-oxo-5-phenyl-valerate	129–138°/ 7 mm	1.4972 (17°)				40.9	C 71.43 H 7.34	C 70.91 H 7.21
Tetrahydro-furfuryl-acetone	Ethyl 3-oxo-5-(2-tetrahydro-furfuryl) valerate	110–117°/ 3 mm	1.4448 (31°)				38	OC_2H_5 23.62	OC_2H_5 21.08

ketone is stable to alkali.

This research is a part of the synthetic study of pyrethrin and cinerin homologues and several 3-methyl-2-cyclopenten-4-ol-1-ones (See Table 2)—some of them are not yet known—have been synthesized by the condensation of methyl glyoxal with these keto esters through the methodes of LaForge et al.[4] or Matsui et al.[5]

Experimental

A. Methyl Ketones

(1) **6-Hepten-2-one.**—Buten-(1)-ol-(4) (b. p. 112-114°) was prepared in 30% yield from allyl bromide and paraformaldehyde, and 4-bromobutene-(1, (b. p. 94-100°) in 64% yield from this butenol by the method of Linstead and Rydon.[6] A solution of sodium methylate prepared by dissolving 12 g. (ca. 0.5 mol.) of sodium in 200 cc. of absolute methanol was cooled to 15° and 70 g. (0.54 mol.) of ethyl acetoacetate was added to the stirred solution. After 1.5 hrs. 68 g. (0.5 mol.) of the above 4-bromobutene was added at once and the reaction was completed by refluxing for five hours. Most of the methanol was removed by distillation and water was added to the residue. Crude ethyl α-3-butenylacetoacetate separated as an upper layer and weighed 57.7 g..

One hundred and thirty eight grams of this crude keto ester and 70 g. of potassium hydroxide in 1.3 l. of water were stirred at 20° for 7 hrs.. The oil was extracted with petroleum ether and discarded. A mixture of 50 cc. of concentrated sulfuric acid and 80 cc. of water was added to the aqueous solution and the mixture was warmed under stirring on a water bath until the evolution of carbone dioxide ceased. The upper oily layer was separated, and the aqueous layer was saturated with sodium chloride and was extracted with petroleum ether. The oil and the petroleum extracts were combined and washed with dilute alkali and saturated sodium chloride solution and dried with potassium carbonate. After evaporation of the solvent, the residue was distilled. 6-Hepten-2-one distilled at 145-150°, yield 42 g. (50 % of the theory based on the crude ester)

(2) **Piperonylacetone.**—One hundred fifty grams of piperonylideneacetone was dissolved in

(4) M. S. Schechter, N. Green and F. B. LaForge, *J. Am. Chem. Soc.*, **71**, 3165 (1949).
(5) M. Matsui, T. Kato et al, *J. Chem. Soc. Japan, Pure Chem. Sect.*, **71**, 235 (1950).
(6) *J. Chem. Soc.*, **1934**, 1993
(7) Kaufmann and Radosevic, *Ber.*, **49**, 679 (1916).
(8) F. B. LaForge et al., *J. Am. Chem. Soc.*, **70**, 3708 (1948).

Table 2

2-Substituted 3-methyl-2-cyclopenten-4-ol-1-ones

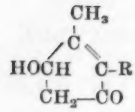

	b. p.	n_D	yield %*	Analytical Data
Methyl	108–110°/ 0.29 mm.	1.5079/ 26°	31	Found: C, 68.01; H, 7.85. Calcd. for $C_7H_{10}O_2$: C, 66.67; H, 7.92%.
Ethyl	132–135°/ 1.3 mm.	1.5082/ 28.5°	30.8	Found: C, 68.40; H, 8.37. Calcd. for $C_8H_{12}O_2$: C, 68.57; H, 8.57%.
Allyl	132–135°/ 1 mm.	1.5141/ 25°	34	Semicarbazone, m. p. 210° Found: C, 56.73; H, 7.20. Calcd. for $C_{10}H_{15}O_2N_3$: C, 57.40; H, 7.23%.
Methallyl	121–126°/ 0.2 mm.	1.5120/ 12°	24	Semicarbazone, m. p. 208–209° Found: C, 59.10; H, 7.25; N, 19.01. Calcd. for $C_{11}H_{17}O_2N_3$: C, 59.19; H, 7.68; N, 18.83%.
2-Butenyl (trans-cinerolone)	127–132°/ 0.5 mm.	1.5096/ 18.5°	45	Semicarbazone, m. p. 208–209° Found: C, 59.79; H, 7.53; N, 19.28. Calcd. for $C_{11}H_{17}O_2N_3$: C, 59.19; H, 7.68; N, 18.83%.
3-Butenyl	126–132°/ 0.5 mm.	1.5151/ 18°	41	Semicarbazone, m. p. 187° Found: C, 59.73; H, 7.40; N, 19.09. Calcd. for $C_{11}H_{17}O_2N_3$: C, 59.19; H, 7.68; N, 18.83%.
Benzyl	161–165°/ 0.15 mm.	1.5680/ 21°	20	Semicarbazone, m. p. 215–216°. Found; C, 64.79; H, 6.48; N, 16.41. Calcd. for $C_{14}H_{17}O_2N_3$: C, 64.87; H,6.56; N, 16.23%.
Piperonyl	146–150°/ 0.23 mm.	1.5670/ 23°	21	Found: C, 68.84; H, 5.21. Calcd. for $C_{14}H_{14}O_4$: C, 68.29;H, 5.59%.
Furfuryl	140–143°/ 0.6 mm.	1.5352/ 16°	38	Semicarbazone, m. p. 201–202° (from ethanol). Found: C, 56.98; H, 6.79; N, 16.97. Calcd. for $C_{12}H_{15}O_3N_3$: C, 57.83; H, 6.02; N,1 6.86%. 3,5-Dinitrobenzoate, m. p. 168–169° Found: C, 55.71; H, 4.28; N, 7.18 Calcd. for $C_{18}H_{14}O_8N_2$: C, 55.95; H, 3.65; N, 7.25%. p-Nitrobenzoate, m. p. 108–109° Found: C, 63.38; H, 4.94; N, 4.10. Calcd. for $C_{18}H_{15}O_6N$: C, 63.34; H, 4.43; N, 4.16%.
Tetrahydrofurfuryl	113–120°/ 0.1 mm.	1.5095/ 19°	4	Found: C, 68.15; H, 7.06. Calcd. for $C_{11}H_{16}O_3$: C, 67.35; H, 8.16%.

* The yields are based on the ester used.

300 cc. of ethyl acetate and reduced with an equivalent amount of hydrogen at 10 atm. in the presence of 10 g. of Raney nickel at room temperature to piperonylacetone, b. p. 152-158°/5 mm. (the reported b. p. 164-5°/12 mm.[7]), yield 105 g. (71% of theory).

(3) Tetrahydrofurfurylacetone.

(i) Tetrahydrofurfurylpropanol-(2). Two hundred and eighty grams of furfurylidene acetone was hydrogenated with 4 equivalent molecules of hydrogen at 40 atm. in the presence of 25 g. of Raney nickel together with some water at 90-120°. The product, boiling 122-131°/24 mm., n_D^{22} 1.4519, was collected, yield 175 g. (62% of theory) (Found: C, 66.14; H, 10.88. Calcd. for $C_9H_{16}O_2$: C, 66.66; H, 11.11%.)

(ii) Tetrahydrofurfurylacetone. Seventy-two grams of tetrahydrofurfuryl-propanol was oxidized with a mixture of 49 g. of potassium bichromate, 70 g. of concentrated sulfuric acid and 250 cc. of water at 60°. The product was extracted with ether. After distillation 31 g. of tetrahydrofurfurylacetone, boiling at 112-115°/28 mm., n_D^{27} 1.4414, was obtained; 2,4-Dinitrophenylhydrazone, yellow crystal, m. p. 76.5°-78.5°C. (Found: N, 17.51. Calcd. for $C_{14}H_{18}O_5N_4$: N, 17.34%).

B. β-Keto-Esters

The general procedure is as follows: one mol. of a methyl ketone is added at a time under stirring to about 3 mols. of sodamide in 1 l. of dry ether at 0° in an ice bath; after 15 minutes the bath is removed and stirring is continued another one hour and then refluxed 15 minutes in a water bath. The bath is replaced by the ice bath and about three mols. of diethyl carbonate is dropped as rapidly as possible. Stirring and refluxing is continued for 4 hours. After cooling three mols. of glacial acetic acid is added and then 600 cc. of water. The upper ether layer is separated and the ether is recovered by distillation. The residual oil is dissolved in an equal volume of petroleum ether and washed several

times with an equal volume of water in order to remove a small quantity of urethan. The urethan can be recovered by extracting the water solution with ether. The petroleum ether solution is dried on anhydrous sodium sulphate or magnesium sulphate. After evaporation of the petroleum ether, the β-keto ester is distilled under reduced pressure.

Summary

A new procedure for preparing β-keto esters from methyl ketones, sodamide and diethyl carbonate using these reagents in the molar ratio of 1:3:3 is reported. The yields of β-keto esters approach to those of the preparation using sodium hydride as condensing agent. Furthermore, some cyclopentenolones were prepared from the β-keto esters synthesized by this procedure.

We are greatly indebted to Dr. Ryo Yamamoto for the valuable advices and to the Ministry of Education for research grants of 1950.

Laboratory of Sumitomo Chemical Co. Ltd. Osaka

The Co-ordinate Compounds of Iron with Some Hydroxycarboxylic Acids

By Kazuo SHIBATA and Tazuhiko NOGUCHI

(Received August 18, 1952)

Sulphosalicylic acid has widely been used for the colorimetric determination of ferric iron in solutions, but of the details of physicochemical properties of the complex formed by co-ordination of hydroxycarboxylic acid of this sort we have only rudimentary information at present. The present work was carried out with the purpose of clarifying some properties of co-ordinate compounds of tri-valent iron with sulphosalicylic acid and related substances, dealing in particular with the determination of the number of ligands chelating with iron and the equilibrium constants between them. The compounds studied were salicylic, sulphosalicylic and 2-hydroxy-3-naphthoic acids, which all, with their hydroxyl group situated in the ortho position to the carboxyl group, form stable complexes with iron.

Methods

The concentration of the complexes formed in solutions was determined spectrophotometrically, using an Adam Hilger monochrometer for visible region combined with the photo-multiplier-tube 931-A. The thickness of the cell compartments used was 1 cm. The mixture of ethanol and water (1:1 in volume) was generally used as the solvent, the purpose of which was to prevent the precipitation of the complexes formed. The standard solution of iron was prepared by dissolving pure iron wire into dil. hydrochloric acid by heating. The ferrous ion in the solution was oxidized by $KClO_3$.

The reaction between acids and iron was observed by the following procedure. 5 cc. of the alcoholic solution of hydroxycarboxylic acid was added to 5 cc. of ferric iron aq. solution. After a while, the absorbance, $E=\log_{10}I_0/I$ (I_0, incident light; I, transmitted light) of the solution was observed at the wave-length of the absorption maximum of the complex formed. As the equal amounts of solutions were mixed together, the solution at the beginning of reaction contained half the concentrations of each component in the original solution, which were denoted by C_f (concentration of iron in g. atoms/l.) and C_h (concentration of hydroxycarboxylic acids in mol./l.), respectively.

Results

(1) **Determination of the Number of Chelating Ligands.**—By a preliminary experiment it was confirmed that the positions of absorption maxima shown by the complexes of sulphosalicylic acid, salicylic acid and 2-hydroxy-3-naphthoic acid were 5100 Å., 5300 Å. and 5900 Å., respectively, in 50% ethanol aq. solution. For sulphosalicylic acid, the absorption maximum was measured in water, which was found to be 4900 Å. The absorbance E of the reaction mixtures was measured using monochromatic light corresponding to the absorption maximum of each complex.

Using a definite concentration of iron solution

($C_f = 0.91 \times 10^{-3}$) the change of E in function of C_h was followed. The experimental curves shown in Fig. 1 indicate that at lower concentrations of C_h, E is proportional to C_h, but with the increase of C_h, E increases more slowly and finally reaches a constant value. It was confirmed that the maximum value of E did not increase any more, even when solid hydroxycarboxylic acid was added to the mixture.

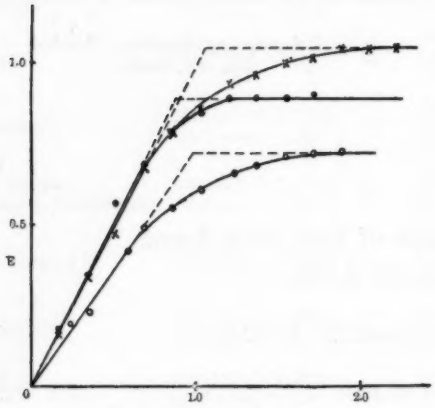

C_h in 10^{-3} mol./l. unit.
● Sulphosalicylic acid
× 2-Hydroxy-3-naphthoic acid
○ Salicylic acid

Fig. 1.

It is obvious that, in the region of linear proportionality, almost all of the hydroxycarboxylic acid added had co-ordinated with iron, while after reaching a constant value of E, almost all of the iron ion was bound. Hence, the value of C_h at the crossing point of the two dotted extrapolated lines shown in Fig. 1 must indicate the upper-most quantity of hydroxycarboxylic acid which can chelate with all iron ions present. These values of C_h were found to be 0.98 for salicylic acid, 0.90 for sulphosalicylic acid and 1.05 for 2-hydroxy-3-naphthoic acid, which all coincide with the value of C_f within the experimental error. A similar experiment was carried out with sulphosalicylic acid, using pure water as solvent. Also in this case, the molecular ratio of chelating agent to iron was found to be one to one.

In Fig. 2 are shown the results of experiments in which the change of E in function of C_f at a definite value of C_h (4.0×10^{-3}) was determined. The distinct linear ascent of the curves shows that under the conditions studied all iron ions have been bound by hydroxycarboxylic acids. The values of tangents of these lines also indicate that the combinations occur at the ratio of one to one.

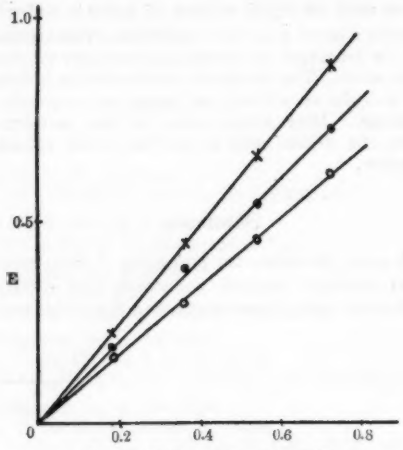

C_f in 10^{-3} g.-atoms/l. unit.
● Sulphosalicylic acid
× 2-Hydroxy-3-naphthoic acid
○ Salicylic acid

Fig. 2.

(2) The equilibrium constant between iron and hydroxycarboxylic acids.—In so far as Beer's law holds, the concentration of a complex in solution must be proportional to the absorbance E of the solution; namely,

$$E = A[\mathrm{HFe}] \tag{1}$$

where (HFe) stands for the concentration of chelated compounds and A for the proportionality constant. The value of A may be estimated either from the value of C_f and the maximum value of E in the experiment shown in Fig. 1, or from the tangent of straight lines in Fig. 2. The values of A thus obtained were 850 for salicylic acid, 1020 for sulphosalicylic acid and 1230 for 2-hydroxy-3-naphthoic acid.

Since the number of ligands chelating with one iron ion was found to be one, the equilibrium between the reaction components may be represented by

$$\mathrm{H} + \mathrm{Fe} \rightleftarrows \mathrm{HFe}$$

$$K = \frac{[\mathrm{HFe}]}{[\mathrm{H}][\mathrm{Fe}]} \tag{2}$$

where H represents the molecule of hydroxycarboxylic acid and K the equilibrium constant. Since C_f and C_h are the concentrations at the beginning of reaction, they are

$$C_f = [\mathrm{Fe}] + [\mathrm{HFe}] \tag{3}$$

$$C_h = [\mathrm{H}] + [\mathrm{HFe}] \tag{4}$$

Substituting equations (3) and (4) in equation (2), we get

$$[\mathrm{HFe}]^2 - (C_f + C_h + 1/K)[\mathrm{HFe}] + C_f C_h = 0$$

Dividing this equation by [HFe], we obtain

$$Z \equiv [HFe] + C_f\left(\frac{C_h}{[HFe]} - 1\right) = C_h + \frac{1}{K} \qquad (5)$$

By applying the data shown in Fig. 1 to this equation, the value of K can be calculated; namely, if we plot the values of Z of the left-hand side of equation (5) against the values of C_h, the points must be on a straight line having a slope of unity and the intersection across the ordinate should be $1/K$. As will be seen from Fig. 3, the linear relationship holds satisfactorily except for the cases of very low concentrations. From the reciprocals of the intersections determined by the method of least square, the values of K of salicylic acid and 2-hydroxy-3-naphthoic acid were found to be 13,900 and 10,900, respectively.

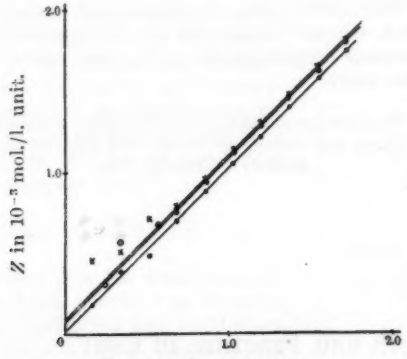

C_h in 10^{-3} mol./l. unit.
● Sulphosalicylic acid
× 2-Hydroxy-3-naphthoic acid
○ Salicylic acid

Fig. 3.

As for the value for sulphosalicylic acid, the intersection was so close to the origin of co-ordinates that the value of K could not be estimated accurately by the above method. Therefore, a resort was had to the following procedure to determine the value in this case. If the mixture contains two kinds of hydroxycarboxylic acids, H_1 and H_2, the equilibrium to be established between them and the iron ion will be;

$$H_1 + Fe \rightleftarrows H_1Fe$$
$$H_2 + Fe \rightleftarrows H_2Fe$$

Therefore,

$$\frac{K_1}{K_2} = \frac{[H_1Fe](C_2 - [H_2Fe])}{[H_2F\ ](C_1 - [H_1Fe])} \equiv K' \qquad (6)$$

where

$$C_1 = [H_1Fe] + [H_1]$$
$$C_2 = [H_2Fe] + [H_2]$$

and K' stands for K_1/K_2.

If the concentrations of the H_1Fe and H_2Fe are estimated experimentally, K' can be calculated, and if K_2 is known K_1 may be obtained from K' and K_2.

As the hydroxycarboxylic acid (H_2) with known equilibrium constant (K_2) we used 2-hydroxy-3-naphthoic acid, which was mixed with sulphosalicylic acid (H_1) in 5 cc. of alcoholic solution and this was added to 5 cc. of iron aq. solution. The absorbances of the solution were measured at the two wave-lengths corresponding to the absorption maxima of H_1Fe and H_2Fe. The values of absorbance thus obtained, which may be denoted by E_1 and E_2, respectively, cannot be regarded as being proportional to the concentrations of the corresponding complexes formed, because the two absorption bands are appreciably broad and overlap with each other at both wavelengths. The situation is schematically illustrated in Fig. 4, where the curve I+II is the absorption curve of the solution obtained, which is thought to be the sum of the curves of I and II for H_1Fe and H_2Fe existing in the solution. The actual absorbance, which is proportional to the concentration of each complex is denoted by E_1' and E_2', respectively, in Fig. 4. Therefore, E_1 and E_2 may be reduced to E_1' and E_2' by solving the following equations;

$$E_1 = E_1' + \frac{E_1''}{E_2'} E_2'$$
$$E_2 = E_2' + \frac{E_2''}{E_1'} E_1'$$

where E_1'' and E_2'' are the absorbances of H_2Fe and H_1Fe at the wave-lengths corresponding to the absorption maxima of H_1Fe and H_2Fe, respectively. The ratios E_1''/E_2' and E_2''/E_1', which can be determined experimentally, may be regarded to be constant independent of the concentrations. From the values of E_1' and E_2' thus obtained, the concentrations of H_1Fe and H_2Fe were calculated using the constant A already determined for each complex.

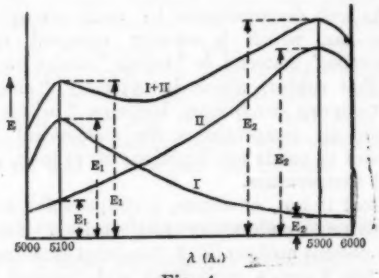

Fig. 4.

Experiments conducted with varying concentrations of H_1, H_2 and Fe, yielded the results shown in Table 1. As may be seen, the value K' calculated from different sets of experiment

showed an excellent agreement, giving a mean value of $K'=2.84$. Since K_2 is 10,900, the value of K_1 (equilibrium constant of Fe-sulphosalicylic acid-complex) is 31,000.

Table 1.

C_1	C_2	C_f	K'
0.720×10^{-3}	0.720×10^{-3}	0.720×10^{-3}	2.76
0.480 〃	0.720 〃	0.480 〃	2.82
0.720 〃	0.480 〃	0.480 〃	2.87
0.688 〃	0.688 〃	0.480 〃	2.90

A similar experiment carried out using salicylic acid and 2-hydroxy-3-naphthoic acid gave the results: (K_1 for salicylic acid):(K_2 for 2-hydroxy-3-naphthoic acid)=1.30. This value coincides fairly well with the value 1.28 calculated from the K-values which have already been determined separately for both substances.

Discussions and Summary

Chelating action of salicylic, sulphosalicylic and 2-hydroxy-3-naphthoic acids towards iron was investigated quantitatively, and it was found that they combine with one-to-one molecular ratio with iron. In order for these substances to be used as colorimetric reagents for the determination of iron, it is desirable that the reagents as well as their complexes be well soluble in water, and that the equilibrium contants of the complexes be sufficiently large so that the proportionality between the absorbance caused by complex and the concentration of iron or chelating agent may hold in a wide range. In this respect sulphosalicylic acid may be regarded as most suitable, among the three hydroxycarboxylic acids studied, as a reagent for iron determination. In view of the fact that the introduction of sulphonyl group into salicylic acid caused the increase of K, it may be expected that a more suitable iron reagents would be obtained by further introduction of sulphonyl group in salicylic acid.

The authors wish to express their thanks to Prof. Hiroshi Tamiya for his guidance and his constant encouragement during the course of this study.

The Tokugawa Institute for Biological Research, Tokyo and Faculty of Science and Engineering, Waseda University, Tokyo

---

Rheology of Coal. IV. Strength and Fracture of Coal

By Katsuya INOUYE and Hideo TANI

(Received July 30, 1952)

Introduction

As well demonstrated by such example as that tar, which is usually accepted as a "ductile" material, is "brittle" under impact, or that rubber, which is typically "elastic" at ordinary conditions, becomes "brittle" at liquid air temperatures, the mechanical properties of solids are functions of, at least, time and temperature.

Coal is not, of course, a simple solid, but is of extreme complexity and variety. One of the present authors (K. I.) has tried experiments on the Young's modulus[1] and internal viscosity[2][3] of coal, which might be able to propose an aspect on the structure and properties of coal from the rheological standpoints, in order to give more straightforward interpretations of the complex properties of coal. As one of the important rheological characteristics of coal, brittleness or strength for rupture is considered in this paper in the light of the facts disclosed in these preceding studies.

The strength of coal is a very important property in various fields of industry concerning coal. First, the mechanical strength is a leading factor for the efficient coal mining, whether the coal is mined by machines or by hands. The fracture of coal during the transportation or coal cleaning is a factor to determine the saleable output rate for definite purposes. The furnace or oven in which the coal is burned or carbonized desires stable

(1) K. Inouye, *J. Colloid Sci.*, **6**, 190, (1951).
(2) K. Inouye, *This Bulletin*, **26** 84 (1953).
(3) K. Inouye, *This Bulletin*, **26**, 157 (1953).

mechanical property of the coal used. There is no doubt of the importance of the strength when the coal is treated in a powdered form, as in floatation, briquetting etc.

In these cases, the coal is subjected to various kinds of stresses, especially varying duration of load. As described above, the coal strength is a function of time, so that the phenomena concerning the strength or fracture should be considered from the standpoint that one cannot speak of a definite characteristic strength of the solid, although some influences of inner flaws and chemical environments in the coal should not be neglected.

F. W. Preston and others[4] have shown, in their experiments on the fatigue of glass that the strength of glass is a simple function of time under a constant load,

$$\log t = -\alpha/m + 1/fm \qquad (1)$$

where, f is the stress required to break a solid, t its duration of application, and α and m are constants. Each sample is thus defined by the inclination factor m (termed fatigue modulus) and by the point t_0, where the line intersects the time axis.

N. W. Taylor[5] has proposed a theory which connects f with t. The slow process preceding fracture is shown to be the orientation of the atomic network contained in an elementary prism of length $r = \lambda_0 E/f$, where E is Young's modulus and λ_0 is the critical elongation required for fracture. The rate-controlling factor is the activation energy, $E\alpha/f$, for the orientation or rearrangement of the atomic network under the stress. The theory has lead to the equations,

$$t = (1/k_0)e^{E\alpha/fKT} \qquad (2)$$

and

$$\log t = -\log k_0 + (E\alpha/2.3\,KT)/f \qquad (3)$$

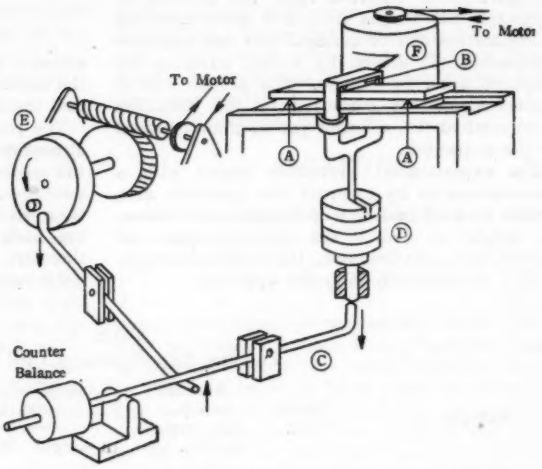

Fig. 1.—Experimental Apparatus

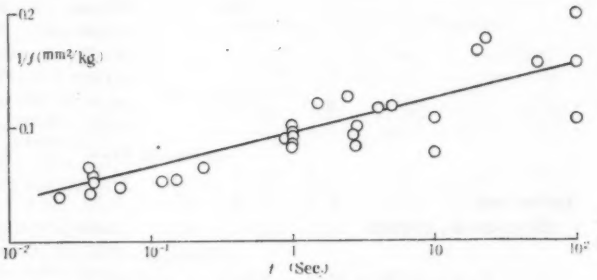

Fig. 2.—$1/f$ versus t for window glass

where K is the Boltzmann constant, T the absolute temperature and α and k_0 are constants. It is noteworthy that the logarithmic expression has the same form as the empirical relation by Preston et al.

The present authors have constructed an apparatus to measure the breaking stress at varying durations of load and, after some preliminary tests with glass in order to check the above-mentioned logarithmic relation between stress and time by their own apparatus, the breaking experiments were carried out on coal to interpret the fracture.

Apparatus and Experimental Procedures

Fig. 1 shows the apparatus schematically. The specimen, cut in a rectangular bar with the accuracy of 1% in each dimension and parallel to the bedding plane, is set on two wedge-shaped metals (A). The stress is applied by another wedge-shaped metal (B) just touched to the centre line in the upper surface of the specimen, when

(4) J. L. Glathart and F. W. Preston, *J. Appl. Phys.*, **17**, 189, (1946).
T. C. Baker and F. W. Preston, *J. Appl. Phys.*, **17**, 170, (1946).
(5) N. W. Taylor, *J. Appl. Phys.*, **18**, 943, (1947).

the shaft (C) is removed from the position of supporting the weight (D). The short duration of application can be changed by a gear and cam mechanism (E) driven by motor, covering the range of 1 sec. to 0.01 sec. The actual time of applied stress was measured by the recording dram method (F), a longer period than 1 second by the stopwatch.

The experimental procedure begins with a measurement to try to break the specimen at a certain time of load, t_1, with continuously changing weight, w, and if the specimen does not fracture at w_m but does at w_n, the breaking strength at t_1, f, is calculated from the equation,

$$f = \frac{3 w_n l}{2 b \tau^2} \qquad (4)$$

where, l is the span length, b the breadth and τ the thickness of the specimen, assuming that the coal fractures is a dynamic solid.

The possible maximum error of the experiment is considered as follows: errors in dimensions of the specimen are ±3%, errors in measuring the weight ±6%, and errors in measuring the time, which however vary with the time range, are ±5% at maximum cases. The total error is, therefore, ±14% at its maximum.

All specimens were examined after being set

Table 1
Fracture Experiments of Coal Samples

Sample	Block No.	Average ash %, dry basis, in vol. (ϕ)	Ash % of specimen (dry basis) in weight	Ash % of specimen (dry basis) in volume (ϕ)	$1/f$ (mm²/kg)	t (sec)
American (Bituminous, strongly-caking)	I	13.0	13.08	8.19	1.28	3×10^{-2}
			19.00	12.34	1.48	1.5
			19.56	12.73	1.54	3.2×10^{-2}
	II	65.0	67.93	55.97	1.18	2×10^{-2}
			69.50	58.57	1.62	1.5
			80.05	70.65	1.52	0.5
			80.07	70.38	1.78	3.5
	III	86.0	90.64	85.32	0.68	300
			91.15	86.07	0.58	4×10^{-2}
			91.37	86.40	0.66	50
			91.56	86.84	0.64	2.5×10^{-1}
Takashima (Bituminous, caking)	I	1.4	2.32	1.41	2.86	2×10^{-2}
			2.33	1.41	3.24	30
			2.37	1.44	2.32	4×10^{-2}
			2.91	1.77	3.90	300
	II	3.0	4.48	2.74	2.24	300
			4.75	2.89	2.00	0.1
			5.03	3.07	1.84	100
			5.49	3.37	2.18	2×10^{-2}
	III	10.0	12.13	7.65	0.84	1.3×10^{-1}
			17.80	11.50	0.64	4.6×10^{-1}
			22.07	14.52	0.98	5
Yubetsu (Producer gas coal)	—	—	22.99	16.61	0.38	1
			27.33	18.41	0.51	4
			28.69	19.42	0.38	4×10^{-2}
			29.43	20.00	0.46	0.5
			29.92	20.39	0.44	10
			31.38	21.53	0.44	3×10^{-2}
			40.63	29.11	0.62	24
			53.15	40.50	0.37	0.2
			55.10	42.41	0.50	3
			57.16	44.46	0.37	5×10^{-2}
			57.83	45.14	0.73	70
Shosaku (Anthracite)	—	3.6	5.64	3.46	1.18	2
			5.72	3.51	1.06	3×10^{-2}
			5.78	3.55	1.12	0.1
			5.83	3.59	1.36	2
			7.21	4.45	1.12	0.1
			7.24	4.47	1.18	2×10^{-2}

into the dessicator of 76% relative humidity for about one month to avoid the influence of the moisture.

Tests on Glass

Approximately 30 specimens were prepared from a piece of window glass and tested by the apparatus. The time for fracture covered the ranges from 5×10^{-2} to 10^3 second. The values of $1/f$, or brittleness index, are plotted against $\log t$ in Fig. 2.

It would appear that the $1/f$ values are more dispersed in the range of longer duration than the shorter. It was, however, assumed that the linear relationship between $1/f$ and $\log t$ is valid in this case. The fatigue modulus, m, obtained using the statistical method is 2.90×10^{-2} mm^2./kg. This value is quite reasonable in comparison with those given by Preston et al.

Brittleness Data of Coals

The coals examined were selected from the same species whose structures were previously discussed in the preceding articles of this study. (For the descriptions of samples, see the reference 2 or 3.)

The brittleness data are given in Table 1 with ash concentrations. The ash contents are recalculated in volume percentages, ϕ, because its significant meaning to the properties has been proposed in the author's preceding reports. Several blocks were chosen for each sample and the specimens were made from each block. After the fracture measurements, the actual ash concentrations were obtained for each specimens, which showed, of course, some deviations; the table also gives the mean values, which were obtained by analyses of mixed powdered samples.

Fatigue Modulus and Activation Energy

The $1/f$ values were plotted against $\log t$ for each block and, assuming the linear relationship between $1/f$ and $\log t$, the fatigue modulus, m, they were obtained from the lines on the graph. The validity of the linear reltionship was better for the anthracite and also the producer gas coal; both showed higher strength and slight deviation in strength with the change of ash concentration than the bituminous coals did. The statistical considerations of the dependence of strength on various factors will be described further in the next paper of this study. Fig. 3 shows the $1/f$ versus $\log t$ relationship for Yubetsu coal. Two values with larger deviation at the durations longer than 10 sec. were omitted from the linear relation.

From Equations (1) and (3),

$$m=2.3\,KT/E\alpha \tag{5}$$

and,

on the other hand, the molal activation energy for fracture is,

$$U=NE\alpha/f \tag{6}$$

where, N= Avogadro's number and hence $NK=R=2$ cal./mol. Therefore, from (5) and (6), U can be calculated from the experimentally known data of m. U values in Table 2 were calculated at first in functions of $1/f$, and then for breaking time of 10^{-2} sec. and 10^2 sec., where T was taken as 288°K (15°C.), the mean room temperature during the experiments.

Table 2

Activation Energy for Fracture

Sample	$m\times10^2$ (mm^2/kg)	$t=10^{-2}$ sec		$t=10^2$ sec	
		f (kg/mm^2)	U (Kcal/mol)	f (kg/mm^2)	U (Kcal/mol)
American					
I	18.9	0.82	8.52	0.53	13.2
II	22.0	0.88	6.88	0.49	12.3
III	2.30	1.71	33.8	1.49	38.7
Takashima					
I	31.8	0.42	10.0	0.28	15.2
II	5.52	0.50	48.0	0.45	53.4
III	11.0	1.52	7.94	0.99	12.2
Yubetsu	2.72	2.69	18.2	2.13	22.5
Shosaku	12.2	1.02	10.7	0.64	16.9

The values of f and U express the strength of coal in absolute units at different ranges of duration of load. It is noteworthy that in each cases the rupture can occur less easily with short time of application of stress than with longer deformation. In other words, the coal can be broken with less force when it is applied a for longer time than at short application. The total molal energy required to

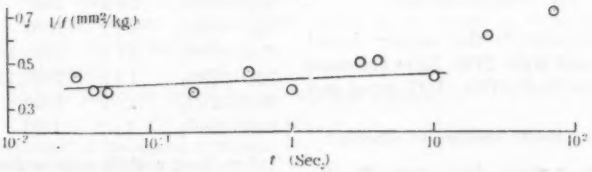

Fig. 3.—$1/f$ versus $\log t$ for Yubetsu producer gas coal.

"activate" the fracture is, however, larger when the deformation is applied for longer duration.

The stress for fracture, f, is larger for the specimen with higher ash concentration (Refer the variations between each result of American coal and of Takashima coal). A remarkable maximum in U values for Takashima coal seems to be difficult to be interpreted; it may be connected with the fact that the Young's modulus of this sample shows a minimum at $\phi=2$ and a maximum at $\phi=8$. (This fact will be reported in detail in Rheology of Coal VI by the present authors.)

The comparison of the strength and the activation energy between species of coals is rather of indefinite conclusion, because of the unequality of analytical composition, although some absolute expressions of industrially empirical strength can be shown.

The comparison of results for Takashima II ($\phi=3.0$) and Shosaku anthracite ($\phi=3.6$) may be interesting; these differences indicate that the bituminous coal is more "brittle" than the anthracite, when applied with stress of short duration, because the ratio of f between the samples is 2.04 at $t=10^{-2}$ sec.; while the difference in strength is slight under long duration of stress, because the ratio is 1.47 at $t=10^{2}$ sec. The comparison of American I ($\phi=13.0$) and Takashima III ($\phi=10.0$) may suggest the fact that the American bituminous coal is of lower strength than the Japanese bituminous coal. These considerations are readily understood if one refers to the results on the Young's modulus and internal viscosity for these coals.[1][2] The detailed discussions with further experimental results will be reported in the next paper.

The authors express their thanks to Dr. M. Kurokawa and Mr. A. Baba for interest in the investigation.

Shigen-Gijyutsu-Shikenjo
(Resources Research Institute)
Saitama-Kawaguchi, Japan

Research on the Crystal Structure of R_3O_5 Type Oxides and Classification of sixfold co-ordinated Oxide Crystals

By Goro YAMAGUCHI

(Received November 7, 1952)

Introduction

The data of crystal structure of pseudo-brookite ($Fe_2O_3 \cdot TiO_2$), a natural mineral, is as follows.[1]

Pseudo-brookite $Fe_2O_3 \cdot TiO_2$ Orthorhombic

$V_h^{17}=$Bbmm $\quad a=9.79$ kX

$Z=4$ $\quad b=9.93$ kX

$\quad c=3.725$ kX

In the previous paper,[2] the author found that $Al_2O_3 \cdot TiO_2$ and $MgO \cdot 2TiO_2$ have the same crystal structure as $Fe_2O_3 \cdot TiO_2$ (R_3O_5 type) and

Table 1

Expected Formula	Mixing Molar Ratio of Powdered Oxides	Sintering Temp. (°C.)	Time (h)	Result*
$Fe_2O_3 \cdot TiO_2$	1 : 1	1250	1	○
$Fe_2O_3SnO_2$	1 : 1	1000, 1250	1	×
$Al_2O_3 \cdot TiO_2$	1 : 1	1250, 1400	1	○
$Al_2O_3 \cdot SnO_2$	1 : 1	1000, 1250	1	×
$MgO \cdot 2TiO_2$	1 : 2	1400	1	○
$MgO \cdot 2SnO_2$	1 : 2	1250	1	×
$CoO \cdot 2TiO_2$	1 : 2	1250, 1400	1	○
$NiO \cdot 2TiO_2$	1 : 2	1250, 1400	1	×
$ZnO \cdot 2TiO_2$	1 : 2	1250	1	○
$ZnO \cdot 2SnO_2$	1 : 2	1250	1	×

* ○···the R_2O_5 type is found by X-rays.
×···the R_2O_5 type is not found.

(1) W. L. Bragg, "Atomic structure of minerals", (1937).
(2) G. Yamaguchi, *J. Ceram. Assoc. Japan*, **55**, 94, (1947).

described a clasification of sixfold coordinated oxide crystals, but, in this paper, other R_2O_5 type oxides and many examples of crystals fitted and not fitted in this classification, shall be described.

Synthetic experiment of R_2O_5 type oxides

Powdered simple oxides were mixed in a definite ratio and sintered at a constant temperature. After cooling, the sintered products were analyzed by X-ray method and their crystal structure was determined. Conditions of synthesis and the results are shown in Table 1, but these conditions are only typical examples of synthesis.

Values of latice constants

Obtained latice constants are shown in Table 2.

Table 2

	Experimental Data (spacing in kX)				Calculated Latice Const		
	d_{662}	d_{436}	d_{322}	d_{220}	a	b	c
$Fe_2O_3 \cdot TiO_2$	1.866	1.969	1.541	2.727	9.80	9.93	3.733
$Al_2O_3 \cdot TiO_2$	1.798	1.905	1.485	2.641	9.46	9.58	3.596
$MgO \cdot 2TiO_2$	1.867	1.978	1.543	2.739	9.84	9.98	3.734
$CoO \cdot 2TiO_2$	1.862	1.960	1.536	2.713	9.75	9.88	3.724
$ZnO \cdot 2TiO_2$	1.867	1.965	1.540	2.723	9.78	9.90	3.734

Table 3

Type	Positive Results	Negative Results.
RO (NaCl or MgO type)	$Li_2O \cdot Fe_2O_3$ (800)*, $Li_2O \cdot Al_2O_3$ (800), $Li_2O \cdot TiO_2$ (1000)	$Li_2O \cdot Cr_2O_3$, $Li_2O \cdot SnO_2$
R_3O_4 (spinel type)	Al_3O_4 (fused),(3) $MgO \cdot Al_2O_3$ (1250), $CoO \cdot Al_2O_3$ (1200), $NiO \cdot Al_2O_3$ (1100), $CuO \cdot Al_2O_3$ (1100), $ZnO \cdot Al_2O_3$ (1100), $MnO \cdot Al_2O_3$ (1100), $MgO \cdot Fe_2O_3$ (1250), $CoO \cdot Fe_2O_3$ (1250), $NiO \cdot Fe_2O_3$ (1250), $Li_2O \cdot 5Al_2O_3$ (800), $Li_2O \cdot 5Fe_2O_3$ (800), $MgO \cdot Cr_2O_3$ (1250), $2MgO \cdot TiO_2$ (1250), $2ZnO \cdot TiO_2$ (1250), $2MgO \cdot SnO_2$ (1250), $2ZnO \cdot SnO_2$ (1250), $2CoO \cdot SnO_2$ (1250), $CoO \cdot MgO \cdot TiO_2$ (1250) [8.43]†, $CoO \cdot ZnO \cdot TiO_2$ (1250) [8.44], $CoO \cdot MgO \cdot SnO_2$ (1250) [8.57], $CoO \cdot ZnO \cdot SnO_2$ (1250) [8.58], $NiO \cdot CoO \cdot TiO_2$ (1250) [8.40], $NiO \cdot ZnO \cdot TiO_2$ (1250) [8.40], $NiO \cdot MgO \cdot SnO_2$ (1250) [8.54], $NiO \cdot ZnO \cdot SnO_2$ (1250) [8.53], $CuO \cdot MgO \cdot TiO_2$ (1100) [8.43], $CuO \cdot CoO \cdot TiO_2$ (1100) [8.43], $CuO \cdot ZnO \cdot TiO_2$ (1000) [8.44], $MnO \cdot MgO \cdot TiO_2$ (1100) [8.46], $MnO \cdot CoO \cdot TiO_2$ (1100) [8.47], $MnO \cdot MgO \cdot SnO_2$ (1250) [8.64], $MnO \cdot CoO \cdot SnO_2$ (1250) [8.66]	$Li_2O \cdot 5Cr_2O_3$, $2NiO \cdot TiO_2$, $2NiO \cdot SnO_2$, $NiO \cdot MgO \cdot TiO_2$, $NiO \cdot CoO \cdot SnO_2$, $CuO \cdot MgO \cdot SnO_2$(?)**, $CuO \cdot CoO \cdot SnO_2$(?), $CuO \cdot ZnO \cdot SnO_2$, $2CuO \cdot TiO_2$, $2CuO \cdot SnO_2$, $MnO \cdot ZnO \cdot TiO_2$, $MnO \cdot ZnO \cdot SnO_2$, $2MnO \cdot TiO_2$,†† $2MnO \cdot SnO_2$
$RO_{4/3\sim3/2}$ (imperfect spinel type)	$MgO \cdot xAl_2O_3$ (sintered or fused), $CoO \cdot xAl_2O_3$ (sintered), $NiO \cdot xAl_2O_3$ (sintered), $Li_2O \cdot yAl_2O_3$ (Sintered) $x > 1$, $y > 5$	
R_2O_3 (Cr_2O_3 type)	$MgO \cdot TiO_2$ (1250), $CoO \cdot TiO_2$ (1250), $NiO \cdot TiO_2$ (1250), $(0.8NiO \cdot 0.2CoO) \cdot TiO_2$ (1250), $(0.9NiO \cdot 0.1CoO) \cdot TiO_2$ (1250)	$CuO \cdot TiO_2$, $MgO \cdot SnO_2$, $NiO \cdot SnO_2$
R_2O_5 ($Fe_2O_3 \cdot TiO_2$ type)	$Fe_2O_3 \cdot TiO_2$ (1400), $Al_2O_3 \cdot TiO_2$ (1400), $MgO \cdot 2TiO_2$ (1400), $CoO \cdot 2TiO_2$ (1400), $ZnO \cdot 2TiO_2$ (1400)	$Al_2O_3 \cdot SnO_2$, $MgO \cdot 2TiO_2$, $Fe_2O_3 \cdot SnO_2$, $MgO \cdot 2SnO_2$, $CoO \cdot 2SnO_2$, $ZnO \cdot 2SnO_2$
RO_2 (SnO_2 type)	TiO_2, SnO_2	

* ( )……one example of sintering temp. (°C) in author's experiment.

† [ ]……latice constant (kX) of spinel which is not listed in "Crystal Structure, Vol. 2" by Wyckoff.

** (?)……doubtful.

†† $2MnO \cdot TiO_2$ is listed as spinel in the Wyckoff's book.

(3) "Aluminium suboxide" G. Yamaguchi, *J. Electrochem. Assoc. Japan*, **14**, 106 (1946); *J. Ceram. Assoc. Japan*, **55**, 42 (1947). *Bull. Chem. Soc. Japan*, **23**, 90 (1952)

Classification of sixfold coordinated oxide crystals and results of synthesis.—Four types of the oxide crystals (RO, R_2O_4, R_2O_3, RO_2) are known, but the author proposes to add the new type, R_2O_5, according to the results of this paper, and the imperfect spinel type ($RO_{4/3\sim3/2}$). The author's extended classification with examples of positive and negative results is as Table 3.

Result

1. Latice constants of R_3O_5 type crystals ($Fe_2O_3 \cdot TiO_2$, $Al_2O_3 \cdot TiO_2$, $MgO \cdot 2TiO_2$, $CoO \cdot 2TiO_2$, $ZnO \cdot 2TiO_2$) are determined.

2. Crystal structures of interoxide compounds of metals, whose coordination number of oxygen is six, are classified into six types; RO(NaCl or MgO type), R_3O_4 (spinel type), $RO_{4/3\sim3/2}$ (imperfect spinel type), R_2O_3 (Cr_2O_3 type), R_3O_5 ($Fe_2O_3 \cdot TiO_2$ type), RO_2 (SnO_2 type). Between interoxide compounds of the same type, formation of solid solution is expected.

3. SnO_2 fits into this theory only in the case of spinel formation.

4. NiO and CuO have almost no acidic property, so that in the cases of formation of R_3O_4 and R_3O_5, they act peculiarly.

5. The author proposes to give the name of "definite ratio solid solution" to crystals of those interoxide compounds when metal atoms are distributed at random at latice points.

Department of Applied Chemistry,
Faculty of Engineering,
the University of Tokyo, Tokyo

LETTER

Phase Transition in the Crystals of Trimethylacetic Acid

By Yoshiyuki NAMBA, Tsutomu ODA and Hisao HAYASHI

(Received December 24, 1952)

In a previous paper,[1] it has been reported that trimethylacetic acid (pivalic acid) crystallizes in a face-centered cubic lattice, the molecules taking orientational or rotational disorder. It has been also optically observed that, on cooling the crystal, it transforms into a birefringent mass. This optical measurement is in harmony with the external observation made by Butlerow[2] who pointed out that this subs ance solidified at the ordinary temperature in a transpa:ent mass, and that when cooled down to about 0°C. it was converted into a snow-like mass. As a continuation of our previous work dilatometric measurements on these transition phenomena and an X-ray study on the structure of the low temperature modification have been carried out.

Dilatometric measurements were made at a temperature range from −20° to 40°C., choosing mercury as the dilatometer liquid. As the result it has been found that the transition is accompanied by abrupt contraction of the volume as the temperature is lowered and occurs really at −2°C., and at 7°C, when the temperature is raised. The relative value of the volume change $\Delta V/V_{18°}$ is approximately 8% and larger than that of fusion. This fact suggests that the transition is accompanied by remarkable enhancement of molecular motion.

In order to confirm this expectation, we prepared complete rotation photographs of single crystals of the low temperature modification, using almost the same method as in the previous paper,[1] except with a cooling apparatus of the Ubbelohde-Woodward type.[3] In this case, as we expected, the intensity of reflection dose not decrease so rapidly with increasing scattering angle as in the high temperature modification. The reflections could not be indexed with the cubic lattice as reported by Butlerow.[2]

Therefore, considering the above mentioned birefringence, this modification should possess

(1) Y. Namba and T. Oda, This Bulletin, **25**, 225(1952).
(2) A. Butlerow, *Ann.*, **173**, 355 (1874).
(3) A. R. Ubbelohde and I. Woodward, *Proc. Roy. Soc.* A, **188**, 358 (1947).

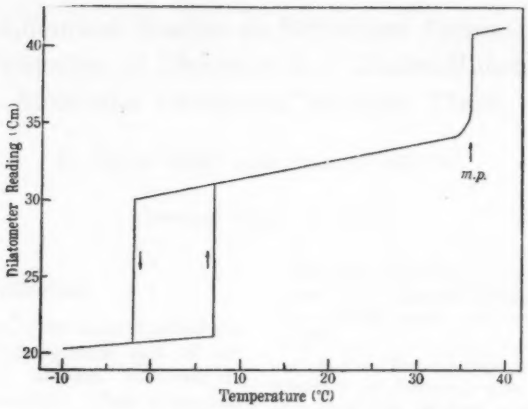

Fig. 1.—Dilatometric curve of $(CH_3)_3CCO_2H$.

a lower symmetry than cubic.

As a conclusion it may be said as ascertained that the intense molecular rotation in the high temperature modification is stopped below the transition and the molecules take an ordered arrangement, in the lattice of low symmetry.

Furthermore, the small changes in volume and entropy[4] at the fusion point indicate that the crystal above the transition temperature may be taken as a good example of organic plastic crystals.[5]

In conclusion, we wish to express our thanks to Professors I. Nitta and S. Seki of the Osaka University for their kind interest throughout this experiment and to Dr. E. Matsumura for his aid in the preparation of the materials.

Chemical Laboratory Osaka Liberal Arts University, Osaka

(4) J. Pirsch, *Ber.*, **70**, 12 (1937).

(5) J. Timmermans, *J. Chim. Phys.*, **35**, 331 (1938).